**Casey, AR, Ruchti, G, Masseron, T, Randich, S, Gilmore, G, Lind, K, Kennedy, GM, Koposov, SE, Hourihane, A, Franciosini, E, Lewis, JR, Magrini, L, Morbidelli, L, Sacco, GG, Worley, CC, Feltzing, S, Jeffries, RD, Vallenari, A, Bensby, T, Bragaglia, A, Flaccomio, E, Francois, P, Korn, AJ, Lanzafame, A, Pancino, E, Recio-Blanco, A, Smiljanic, R, Carraro, G, Costado, MT, Damiani, F, Donati, P, Frasca, A, Jofre, P, Lardo, C, de Laverny, P, Monaco, L, Prisinzano, L, Sbordone, L, Sousa, SG, Tautvaisiene, G, Zaggia, S, Zwitter, T, Delgado Mena, E, Chorniy, Y, Martell, SL, Aguirre, VS, Miglio, A, Chiappini, C, Montalban, J, Morel, T and Valentini, M**

**The Gaia-ESO Survey: revisiting the Li-rich giant problem**



**Article**

Mon. Not. R. Astron. Soc. **000**, 1–24 (2015) Printed 6 August 2016 (MN LATEX style file v2.2)

# The Gaia-ESO Survey: Revisiting the Li-rich giant problem

A. R. Casey[1⋆], G. Ruchti[2], T. Masseron[1], S. Randich[3], G. Gilmore[1], K. Lind[4,5], G. M. Kennedy[1], S. E. Koposov[1], A. Hourihane[1], E. Franciosini[3], J. R. Lewis[1], L. Magrini[3], L. Morbidelli[3], G. G. Sacco[3], C. C. Worley[1], S. Feltzing[2], R. D. Jeffries[6], A. Vallenari[7], T. Bensby[2], A. Bragaglia[8], E. Flaccomio[9], P. Francois[10], A. J. Korn[5], A. Lanzafame[11], E. Pancino[3,12], A. Recio-Blanco[13], R. Smiljanic[14], G. Carraro[15], M. T. Costado[16], F. Damiani[9], P. Donati[8,17], A. Frasca[18], P. Jofré[1], C. Lardo[19], P. de Laverny[13], L. Monaco[20], L. Prisinzano[9], L. Sbordone[21,22], S. G. Sousa[23], G. Tautvaišienė[24], S. Zaggia[7], T. Zwitter[25], E. Delgado Mena[23], Y. Chorniy[24], S. L. Martell[26], V. Silva Aguirre[27], A. Miglio[28], C. Chiappini[29], J. Montalban[30], T. Morel[31], M. Valentini[29]
*Affiliations can be found at the end of this Article.*



Accepted 2016 XX XX. Received 2016 February XX; in original form 2016 May XX

**ABSTRACT**

The discovery of lithium-rich giants contradicts expectations from canonical stellar evolution. Here we report on the serendipitous discovery of 20 Li-rich giants observed during the *Gaia-ESO Survey*, which includes the first nine Li-rich giant stars known towards the *CoRoT* fields. Most of our Li-rich giants have near-solar metallicities, and stellar parameters consistent with being before the luminosity bump. This is difficult to reconcile with deep mixing models proposed to explain lithium enrichment, because these models can only operate at later evolutionary stages: at or past the luminosity bump. In an effort to shed light on the Li-rich phenomenon, we highlight recent evidence of the tidal destruction of close-in hot Jupiters at the sub-giant phase. We note that when coupled with models of planet accretion, the observed destruction of hot Jupiters actually predicts the existence of Li-rich giant stars, and suggests Li-rich stars should be found early on the giant branch and occur more frequently with increasing metallicity. A comprehensive review of all known Li-rich giant stars reveals that this scenario is consistent with the data. However more evolved or metal-poor stars are less likely to host close-in giant planets, implying that their Li-rich origin requires an alternative explanation, likely related to mixing scenarios rather than external phenomena.

**Key words:** stars: abundances

## 1 INTRODUCTION

Lithium is a fragile element which cannot be easily replenished. Given its fragility, canonical stellar evolution models predict that a star's Li abundance should decrease as it ascends the giant branch. Observations since Bonsack (1959) have repeatedly confirmed these predictions. However, Population I stars show lithium abundances approximately ten times higher than older Population II stars, implying some kind of Galactic lithium enrichment. More puzzlingly, there exists a growing number of giant stars with lithium abundances that are near to, or exceed Big Bang nucleosynthesis predictions. Although rare, these stars constitute a fundamental outstanding problem for stellar evolution.

Stellar evolution theory suggests that the depth of the convective envelope increases when a star leaves the main-sequence. In doing so, the star experiences first dredge-up: material from deep internal layers is mixed towards the surface (Iben 1967a,b). The inner material is hot enough that Li has been destroyed, therefore first dredge up dilutes the surface Li abundance. Consequently, stellar evolution theory predicts the observable Li abundance should be ∼1.5 dex

⋆ E-mail: arc@ast.cam.ac.uk

lower for evolved stars than their main-sequence counterparts. (e.g., Iben 1967a; Lagarde et al. 2012) Stars on the upper red giant branch (RGB) may be even more depleted in Li due to mixing occurring just after the RGB bump (Sweigart & Mengel 1979; Charbonnel 1994, 1995). Other changes to surface abundances are also predicted: increases in $^{4}$He, $^{14}$N, $^{13}$C, and decreases in $^{12}$C (Iben 1964; Chanamé et al. 2005; Charbonnel 2006; Charbonnel & Lagarde 2010; Karakas 2010; Lattanzio et al. 2015). Detailed observations have repeatedly provided convincing evidence of these predictions (e.g., Lambert et al. 1980; Spite & Spite 1982; Gratton et al. 2000; Lind et al. 2009b; Mucciarelli et al. 2012; Tautvaišienė et al. 2013).

The existence of Li-rich (A(Li) $\gtrsim$ 2) giant stars implies an additional mechanism that produces and/or preserves surface Li. This process may be internal or external. In the right conditions stars can produce Li internally through the Cameron-Fowler mechanism (Cameron & Fowler 1971): $^{3}\mathrm{He}(\alpha,\gamma)^{7}\mathrm{Be}(e^{-},\nu)^{7}\mathrm{Li}$. The temperature must be hot enough for $^{7}$Be to be produced, but $^{7}$Be must be quickly transported towards cooler regions so that fresh $^{7}$Li can be created without being immediately destroyed by proton capture. The Cameron-Fowler mechanism can operate in red giants in two different stages. During hot bottom burning (HBB), the bottom of the convective envelope is hot enough for $^{7}$Be production. The convection carries $^{7}$Be to cooler regions where it can capture an electron to produce $^{7}$Li. In the absence of HBB, a radiative zone exists between the shell and the convective envelope. A mechanism is then required to mix material down to the outer part of the shell – where temperatures are high enough to produce $^{7}$Be – and then fresh $^{7}$Be must be mixed across the radiative zone to the convective envelope. The mechanism for mixing through the radiative zone is under debate, but various mechanisms are collectively referred to as 'deep-mixing' or 'extra-mixing'. Moreover, because the conditions required to produce $^{7}$Li are also sufficient to destroy it (e.g., by mixing fresh $^{7}$Li back to hotter regions), the level of subsequent Li-enhancement due to extra mixing is critically sensitive to the mixing speed, geometry, and episodicity (e.g., Sackmann & Boothroyd 1999).

Several scenarios have been proposed to reconcile the existence of Li-rich giant stars, including ones that aim to minimise the amount of partial burning (i.e., preserve existing Li). However using *Hipparcos* parallaxes (van Leeuwen 2007) and stellar tracks to precisely estimate stellar masses and evolutionary states, Charbonnel & Balachandran (2000) highlight fifteen Li-rich giants where Li preservation is insufficient: a Li-*production* mechanism is required to match the data. While precise, Li abundance measurements can be limited by the stellar tracks employed (e.g., including the horizontal or asymptotic branch for low-mass stars), emphasising the need for accurate knowledge of the evolutionary status. Charbonnel & Balachandran (2000) propose two distinct episodes of Li production that depend on the stellar mass. For low-mass RGB stars at the bump in the luminosity function, the outward-moving hydrogen shell burns through the mean molecular weight discontinuity produced during first dredge up, enabling extra mixing and facilitating the Cameron-Fowler mechanism. However in intermediate-mass stars, the composition discontinuity is not destroyed until after the star begins core He burning. For this reason extra mixing can only be induced in intermediate-mass asymptotic giant branch (AGB) stars when the convective envelope deepens at the base of the AGB. While these scenarios explain the necessary internal conditions required to produce and transport Li to the photosphere, they do not speculate on the actual mechanism that drives the mixing (however see Charbonnel & Zahn 2007). Palacios et al. (2006) have shown that rotation alone is insufficient to produce the observed Li abundances, implying that an additional mechanism is required to induce the extra mixing.

Thermohaline mixing has been proposed as a mechanism to drive extra mixing at the bump in the giant branch luminosity function. In addition to removing any existing molecular weight gradient, an inversion in the molecular weight gradient is produced, which drives thermohaline mixing (Eggleton et al. 2006). In contrast, Denissenkov & VandenBerg (2003) incorporate diffusion and shear-driven mixing to facilitate extra-mixing in low-mass RGB stars. Their prescription relies on main-sequence stars (as the precursors of upper RGB stars) to possess rapidly rotating radiative cores. Instead of encouraging interactions between different mass shells (e.g., Charbonnel & Balachandran 2000), Denissenkov & VandenBerg (2003) require the specific angular momentum to be conserved in each shell during the star's evolution. This situation would therefore permit a reservoir of angular momentum which could later induce deep mixing.

Palacios et al. (2001) proposed that internal instabilities occurring near the luminosity bump were sufficient to produce additional Li. Specifically, internally-produced $^{7}$Be could be transported to a nearby convective region where $^{7}$Li is produced, but immediately destroyed by proton capture. In effect, a thin burning layer of Li is created, where $^{7}\mathrm{Li}(p,\alpha)\alpha$ becomes the dominant reaction, increasing the local temperature and the level of meridional circulation. The molecular weight gradient is eventually destroyed, allowing for deep mixing to occur. While promising, this scenario requires an arbitrary and substantially large change in diffusion rates. A significant amount of mass-loss is expected as a consequence of this scenario, as well as an excess in infrared colours. Given extensive investigations into the (lack of) association between far infrared excesses and Li-rich giants, it would appear this scenario may be unlikely, unless the infrared excess phase is short (Rebull et al. 2015; de la Reza et al. 2015).

The extra mixing required may be induced by external phenomena. The ingestion of a massive planet or brown dwarf would contribute significant angular momentum to the system, producing additional Li before it is destroyed by convection (Alexander 1967; Siess & Livio 1999a,b; Denissenkov & Weiss 2000; Denissenkov & Herwig 2004; Carlberg et al. 2010). In this scenario the planet is assumed to be dissipated at the base of the convective envelope of a giant star, causing the star to substantially expand in size. If the accretion rate is high, HBB can be triggered. The predicted observational signatures vary depending on the accretion rate and the ingestion angle of the planet/dwarf. However, the predicted observables include increased mass loss and/or the ejection of a shell (and therefore a subsequent phase of infrared emission), an increase in the $^{7}$Li surface abundance, potential stellar metallicity enrichment, possibly increased rotational velocity due to the transfer of angular momentum, and less discernible effects such as the generation of

magnetic fields (however see Lèbre et al. 2009) or changes to the morphology of the horizontal branch. Siess & Livio (1999a,b) argue that the planet/dwarf star accretion scenario is not limited to a single evolutionary stage, allowing for Li-rich giants to exist on the red giant and the asymptotic giant branch. It can also advantageously explain stars with either high or low rotational velocities, depending on the extent that magnetic braking has influenced spin-down. However, there has been no discussion in the literature on how this scenario alone relates to why Li-rich giants tend to appear more frequently just below the RGB bump (e.g., see Figure 1). Similarly, there has been no discussion of links between Li-rich giant stars and the properties or occurrence rates of exoplanet host stars.

Martin et al. (1994) propose a novel external mechanism to reconcile observations of Li-rich giant stars. High Li abundances detected in the secondaries of a stellar-mass black hole (Martin et al. 1992) and neutron star (Martin et al. 1994) candidates led to the postulation that Li could be produced during a supernova explosion (see also Tajitsu et al. 2015), or through $\alpha$-$\alpha$ reactions during strong outbursts from a transient X-ray binary system. These conditions could be sufficiently energetic to induce cosmic-ray spallation and produce Li (Walker et al. 1985). Li would presumably be accreted to the edge of the convective envelope of the secondary thereby producing a Li-rich giant star, potentially at any stage across the RGB, with low rotational velocities. A consequence of Li spallation is that beryllium and boron would also be created. To date, no Li-rich giant star has been found to have Be enhancement (de Medeiros et al. 1997; Castilho et al. 1999; Melo et al. 2005). Finally, although no long-term radial velocity studies have been conducted, the non-detection of a white dwarf companion in the vicinity of a present-day Li-rich giant star weakens this idea.

Observations have been key to guiding models that can explain Li-rich giant stars. Unfortunately most Li-rich giant stars are not distinguishable by their photometric colours, therefore they cannot be efficiently selected solely on the basis of photometry. Early observations of far-infrared colours showed that many Li-rich stars show far-infrared excesses (de La Reza et al. 1996, 1997), suggesting that the Li-rich phase was associated with a mass-loss event. However later K-giant selections based on far-infrared colour excesses did not reveal any new Li-rich stars (Fekel & Watson 1998; Jasniewicz et al. 1999). Rebull et al. (2015) studied this phenomenon extensively and revealed that the largest infrared excesses do indeed appear in Li-rich K giants (typically with fast rotation, see also Fekel & Balachandran 1993), although very few Li-rich K giants show any infrared excess. Kumar et al. (2015) came to the same conclusion from a study of $\sim$ 2000 K giants. Therefore, if mass-loss or dust shell production is a regular consequence of the Li-enrichment mechanism, the infrared excess phase must be short (de la Reza et al. 2015).

Discoveries of Li-rich giant stars have been slow relative to advances in modelling. Their sparsity is partly to blame: only 1% of slow rotating K giant stars are Li-rich (although $\sim$50% of rapid rotating K giants are Li-rich, see Drake et al. 2002; Lèbre et al. 2006). For this reason most discoveries have been reported individually, although they cover all major components of the Galaxy: towards the bulge (McWilliam & Rich 1994; Uttenthaler et al. 2007; Gonzalez et al. 2009), disk (Monaco et al. 2011), as well as plenty in the field[1]. Li-rich giant stars have also been found in dwarf galaxies (Kirby et al. 2016), where the most metal-poor ([Fe/H] $\approx -2.8$) Li-rich giant star known has been found (Kirby et al. 2012). Interestingly, despite large observational programs dedicated to obtaining high-quality spectra in clusters, fewer than ten Li-rich giants have been discovered in globular clusters (2 in NGC 362, M3-IV101, M5-V42, M68-A96, etc; Smith et al. 1999; D'Orazi et al. 2015; Kraft et al. 1999; Carney et al. 1998; Ruchti et al. 2011; Kirby et al. 2016), and just five in open clusters (NGC 7789-K301, Berkeley 21, M 67, Trumpler 5, and NGC 6819; Pilachowski 1986; Hill & Pasquini 1999; Canto Martins et al. 2006; Monaco et al. 2014; Anthony-Twarog et al. 2013; Carlberg et al. 2015, respectively)[2].

Because the mixing mechanisms required to produce Li-rich giant stars are sensitive to the evolutionary stage, asteroseismology is a promising field to distinguish proposed mixing scenarios. To date five Li-rich giant stars have been discovered in the *Kepler* field (Martell & Shetrone 2013; Silva Aguirre et al. 2014; Jofré et al. 2015; Anthony-Twarog et al. 2013; Carlberg et al. 2015). However only two have benefited from seismic information. One Li-rich giant star has been shown to host a He-burning core, suggesting that Li production may have occurred through non-canonical mixing at the RGB tip (Kumar et al. 2011), possibly during the helium flash (see also Cassisi et al. 2016). In contrast, seismic data for the Li-rich star KIC 9821622 has shown that it does *not* host a He-burning core, and sits just before the luminosity bump on the giant branch (Jofré et al. 2015). Clearly, a larger sample of Li-rich giant stars with detectable solar-like oscillations is needed.

Large scale spectroscopic surveys are ideal vehicles for increasing the sample of known Li-rich giant stars. In this *Article* we report the serendipitous discovery of 20 previously unknown Li-rich giants in the *Gaia-ESO Survey*. Four were observed with the UVES spectrograph, and the remainder using GIRAFFE. This constitutes one of the largest sample of Li-rich giant stars ever discovered. This *Article* is organised in the following manner. In Section 2 we describe the data and analysis. We discuss the evolutionary stage and associated environments for all stars in our sample in Section 3, before commenting on the likelihood of different Li production mechanisms. We conclude in Section 4.

## 2 DATA & ANALYSIS

The *Gaia-ESO Survey* (Gilmore et al. 2012; Randich et al. 2013, ESO programs 188.B-3002 and 193.B-0936) is a $\sim$300-night program that simultaneously uses the UVES and GIRAFFE spectrographs (Dekker et al. 2000; Pasquini et al. 2000) on the Very Large Telescope in Chile to obtain high-resolution optical spectra for >100,000 stars in the Galaxy. Targets from all stellar populations are observed.

[1] For example, see Wallerstein & Sneden (1982); Luck (1982); Hanni (1984); Andrievsky et al. (1999); Balachandran et al. (2000); Reyniers & Van Winckel (2001); Lèbre et al. (2009); Alcalá et al. (2011); Kumar et al. (2011); Ruchti et al. (2011); Kővári et al. (2013); Liu et al. (2014); Adamów et al. (2015).

[2] See also Delgado Mena et al. (2015).

We searched the fourth internal data release (iDR4) of the *Gaia-ESO Survey* for giant stars with peculiarly high lithium abundances. We restricted our search to K-type giant stars with Li measurements (i.e., not upper limits) where A(Li LTE) $\gtrsim 2$. Our search revealed 4 bonafide Li-rich giant stars observed with UVES, and 16 observed with GIRAFFE. A cross-match of the *Survey* observing logs reveals these spectra were obtained in good seeing (0.6-0.9″) throughout 2013-2014. Standard data reduction procedures were employed, as detailed in Sacco et al. (2014) and Lewis et al. (2016). The S/N of the spectra range from ≈30 to ≈100.

The *Gaia-ESO Survey* employs multiple analysis pipelines to produce a robust ensemble measurement of the stellar parameters (Table 2: $T_{\rm eff}$, $\log g$, [M/H]) and detailed chemical abundances. The analysis of FGK-type stars within the *Survey* is split between different working groups (WGs): WG10 analyses FGK-type stars observed with GIRAFFE, WG11 analyses FGK-type stars observed with UVES (Smiljanic et al. 2014), and WG12 analyses pre-main-sequence candidates (Lanzafame et al. 2015) – irrespective of whether they were observed with GIRAFFE or UVES. Within each WG there are multiple analysis nodes. A node consists of a sufficiently distinct pipeline, and expert spectroscopists that are familiar with the pipeline employed. All nodes provide estimates of the stellar parameters and/or detailed chemical abundances. For the *Gaia-ESO Survey* iDR4, there are up to six nodes for WG10, and eleven for WG11.

There are some commonalities between the nodes. The MARCS 1D model atmospheres (Gustafsson et al. 2008) are used by all nodes, the same atomic line data (Ruffoni et al. 2014; Heiter et al. 2015) and solar abundances (Grevesse et al. 2007) are employed, and where relevant, the same grid of synthetic spectra is used. The WG10/GIRAFFE nodes are provided initial guesses of the stellar parameters from a preprocessing pipeline. The data reduction procedure also produces normalised spectra for all nodes, however some nodes opted to repeat or redo the normalisation.

The spectral analysis is performed in two consecutive stages. The stellar parameters reported by each node are homogenised to produce an ensemble measurement of stellar parameters for a given star. Those homogenised measurements are then returned to the nodes, at which point the detailed chemical abundances are calculated using the homogenised stellar parameters. Appropriate data are accounted for during the abundance determination of each line or element (e.g., hyperfine structure, the Fe 6707.4 Å blend for Li abundances, etc). Individual abundances are subsequently homogenised, producing a single set of abundance measurements for all co-investigators of the *Survey* to use. In both stages (stellar parameters, chemical abundances), the homogenisation procedure identifies erroneous node measurements, accounts for the covariance between sources of measurements, and quantifies or minimises systematics present in the data. Most critically, the top-level homogenisation (performed by WG15) ensures that results from multiple WGs are on a consistent, comparable scale. Details of the analysis nodes, work structure and homogenisation procedure for the previous WG11 data release is presented in Smiljanic et al. (2014). A full description of the homogenisation procedure for UVES iDR4 data will be presented in Casey et al. (2016).

### 2.1 Characterisation and Evolutionary Status of Li-Rich Stars

Our sample of bonafide Li-rich giant stars includes targets analysed by WG10, WG11, and WG12. While the WG12 group include experts on the analysis of pre-main-sequence stars, they are also specialists in standard FGK-type star analyses. This is important to note, as not all stars targeted by WG12 are later found to be pre-main-sequence stars; some stars targeted by WG12 are actually standard FGK-type stars. Half (10) of our Li-rich giant stars were analysed by WG10 or WG11. The remainder were targeted as pre-main-sequence candidates towards young clusters, but were later found to be giant stars that are likely non-members of those clusters (see below). Their evolved nature is indicative from their stellar parameters, the empirical $\gamma$-index (we required $\gamma > 1.01$; Damiani et al. 2014), and lack of H-$\alpha$ emission (a youth indicator for pre-main-sequence stars).

Most stars in our sample lie below the RGB bump (Figure 2), consistent with previous studies of Li-rich giant stars with near-solar metallicities (Figure 1). Some stars are exceptions: 18033785–3009201 was observed with UVES and lies just above the RGB bump, near the clump. 19230935+0123293 has a similar surface gravity, but is hotter and more consistent with being a red clump (RC) or AGB star. 19301883–0004175 is the coolest and most metal-poor ([Fe/H] $= -0.52$) Li-rich giant star in our sample. Our stellar parameters place 19301883–0004175 slightly red-ward (below) of the isochrone. Given this star is in the *CoRoT* field, combining asteroseismic oscillations with the high-quality *Gaia-ESO Survey* spectra would be advantageous to firmly establish the evolutionary state of this highly evolved Li-rich giant star.

The *Gaia-ESO Survey* reports individual chemical abundances for up to 45 species in iDR4: 34 elements at different ionisation stages. These range from $Z = 3$–$63$ (Li to Eu) and include odd-Z, $\alpha$-, Fe-peak, as well as neutron-capture ($s$- and $r$-process) elements. The resolution, wavelength coverage, and S/N of the GIRAFFE sample is inferior to UVES, therefore only a maximum of 15 species are available from GIRAFFE spectra. Given the S/N and spectral type of our Li-rich giant sample, for some stars we report abundances for only a few (or no) elements. Tables 3-5 contain the detailed abundances for all Li-rich giants in our sample. We find no obvious anomalous pattern in the detailed chemical abundances of our Li-rich stars (Figure 3). This confirms findings from other studies that conclude Li seems to be the only element of difference (e.g., Ruchti et al. 2011; Martell & Shetrone 2013). For completeness purposes we have calculated non-LTE lithium abundances using the grid of corrections from Lind et al. (2009a). These measurements are listed in Table 5, but throughout this text all abundances refer to those calculated in LTE.

There is little doubt that these stars are indeed Li-rich. In Figure 4 we show the spectra surrounding the Li resonance doublet at 6707 Å and the subordinate line at 6103 Å for the Li-rich stars observed with UVES. A comparison giant star of similar stellar parameters is shown in each panel, highlighting the difference in Li. The 6707 Å line is strong in all four stars and saturates in the bulge star 18033785–3009201. The 6103 Å line is also visible. Similarly, we show the 6707 Å line for all Li-rich stars observed with GIRAFFE

in Figure 4, confirming their high Li abundances. The 6103 Å line is not covered by the GIRAFFE setups employed.

We find only one Li-rich giant star in our sample to be a fast rotator ($v \sin i \gtrsim 20$ km s$^{-1}$): 11000515-7623259, the star towards Chameleon 1. We find no evidence of binarity in our sample: no significant secondary peak is seen in the cross-correlation function, and no spectral lines are repeated. However this does not preclude the possibility of a faint binary companion. Repeat radial velocity measurements over a long baseline may be required to infer the presence of any companion.

We searched for indications of significant mass-loss in our sample of Li-rich stars. We cross-matched our sample with the Wide-Field Infrared Survey Explorer (hereafter WISE, Wright et al. 2010) and the 2 Micron All Sky Survey (2MASS, Skrutskie et al. 2006) catalogues to search for infrared excesses that may be attributable to ejected shells or dust-loss. All stars had entries in 2MASS and WISE. We investigated all possible combinations of near- and mid-infrared colours and found no significant difference in the colours (or magnitudes) of our Li-rich stars. Two stars exhibited mild excesses in WISE colours, but there are indications that the reported excess is due to source confusion and high background levels. If the Li-rich stars in our sample are experiencing significant mass-loss as dust, that signature may only be observable in the far infrared. Because these stars are (relatively) faint (see Table 2), they may not be visible in the far infrared even if a substantial relative excess exists due to the presence of a shell.

Giant stars experiencing significant mass-loss as gas often show blue-ward asymmetry in their H-$\alpha$ profile (e.g., Mészáros et al. 2009). Figure 5 shows spectra for all Li-rich giant stars around the H-$\alpha$ line. No obvious asymmetry is present for the UVES sample. There is some suggestion of asymmetry in some of the GIRAFFE Li-rich giants, most notably 08102116-4740125 and 11000515-7623259. However for most Li-rich stars in our sample, there is weak evidence for any recent and significant mass loss, either in the form of gas, dust, or shells.

## 3 DISCUSSION

The key to understanding the nature of the Li production and preservation mechanisms in giant stars is to accurately know their evolutionary stage and the surrounding environment. Although some of our Li-rich stars have evolved past the RGB bump, the majority of our Li-rich giants lie just below the RGB bump. This is consistent with other studies of Li-rich giants of solar-metallicity (e.g., Martell & Shetrone 2013, and Figure 1), whereas most metal-poor Li-rich giants have been found at more evolved stages: either slightly past the RGB bump (e.g., D'Orazi et al. 2015), towards the RGB tip, red clump, or on the AGB (e.g., Kumar et al. 2011; Ruchti et al. 2011).

The fact that many of our stars lie before the RGB bump is a genuine problem, because this is before the discontinuity in mean molecular weight can be destroyed, irrespective of mass. An alternative scenario is that these stars have simply been mis-classified as pre-bump stars (e.g., da Silva et al. 2006), and they are more likely past the luminosity bump or are red clump stars.

Below we discuss the observational signatures, the evolutionary stage, environment and membership thereof for all Li-rich giant stars in our sample, before commenting on the plausibility of the proposed scenarios.

### 3.1 Environment & Evolution

#### *3.1.1 Li-rich giants towards clusters*

Half of our Li-rich stars are in the direction of open clusters. This is due to an observational bias: the GIRAFFE instrument setups used for the *Gaia-ESO Survey* Milky Way fields do not include the Li line. Additional setups are used for clusters and special fields (e.g., the *CoRoT* fields), which include Li. The clusters surrounding each Li-rich star are shown in Table 2. Below we discuss why these Li-rich giant stars are unlikely to be bonafide cluster members. However, we stress that our conclusions are not conditional on (non-)membership for any of the Li-rich giant stars. While cluster membership clearly has an influence on the frequency of Li-rich giant stars in the field and clusters (Section 3.3), these inferences are similarly complicated by the absence of quantifiable selection functions for other Li-rich giant studies.

We find two Li-rich giants towards the young open cluster gamma2 Velorum, neither of which are likely members. 08102116-4740125 has a radial velocity that is inconsistent with the cluster, and 08095783-4701385 has a velocity near the maximum cluster value (26 km s$^{-1}$). More crucially, any giants towards *any young cluster* like gamma2 Velorum (5-10 Myr) are extremely unlikely to be cluster members given the cluster age. This reasoning extends to 08395152-5315159 towards IC 2391 (53 Myr), the Li-rich giants towards NGC 2547 (35 Myr) and Chamaeleon 1 (2 Myr), and the four Li-rich giant stars towards IC 2602 (32 Myr).

This argument does not extend to NGC 6802, which is substantially older (1 Gyr). Nevertheless, the UVES Li-rich star towards NGC 6802 is also unlikely to be a bonafide member. Janes & Hoq (2011) classify it as a likely non-member in their detailed cluster study, and Dias et al. (2014) estimate a 66% membership probability based on proper motions. The radial velocity is mildly ($\sim 2\sigma$) inconsistent with the distribution of cluster velocities. Finally, the metallicity places 19304281+2016107 a full 0.2 dex lower than the cluster mean, significantly away from the otherwise small dispersion in metallicity seen for this cluster.

#### *3.1.2 18033785-3009201, the Li-rich bulge star*

The discovery of 18033785–3009201 at $(l, b) = (1^\circ, -4^\circ)$ makes it the most Li-rich giant star known towards the bulge (McWilliam & Rich 1994; Gonzalez et al. 2009). Its radial velocity ($-70$ km s$^{-1}$) is consistent with bulge membership for stars at this location (Ness et al. 2013).

The detailed chemical abundances we derive are in excellent agreement with the literature. Bensby et al. (2013) report detailed chemical abundances from 58 microlensed dwarf and sub-giant stars in the bulge. A comparison of their work with respect to 18033785–3009201 is shown in Figure 6. Although we find slightly higher [Na/Fe] and [Al/Fe] ratios than Bensby et al. (2013), our abundances are consistent with other bulge studies focusing on giant stars (e.g., Fulbright et al. 2007).

18033785–3009201 exhibits a noteworthy deficiency in the classical *s*-process elemental abundances: Ba, La, Ce, Pr, and Nd. Although the uncertainty on Pr II is quite large ($\sim$0.5 dex), on average we find 18033785–3009201 to be depleted in *s*-process elements relative to iron, by $\sim$0.3 dex. This signature is not seen in the classical *r*-process element Eu, where we find [Eu/Fe] $= 0.05 \pm 0.10$ dex. Low [*s*-process/Fe] abundance ratios are generally consistent with an ancient population (e.g., dwarf galaxies, however there are exceptions), and the depletion in these elements firmly rules out any scenarios where the increased surface Li abundance is associated with mass transfer from a nearby companion, which would result in an increase of [*s*/Fe] abundance ratios.

The stellar parameters for 18033785–3009201 place it near the RGB bump. Given the uncertainty in $\log g$, we cannot rule out whether this star is on the RGB or is actually a red clump star. The measured [C/O] ratio of 0.03 is near-solar, and while this is only weak evidence, it suggests the star has not completed first dredge up as a decrease in C abundances would be expected (e.g., Karakas & Lattanzio 2014). A better understanding of the evolutionary state would be useful to constrain the details of any internal mixing. However we note that detecting asteroseismic oscillations from 18033785–3009201 is not likely in the foreseeable future, as its position lies 2° from the closest planned *K2* field[3] towards the bulge.

#### *3.1.3 Li-rich giants in the CoRoT field*

Our sample contains the first Li-rich giant stars discovered towards any *CoRoT* fields. One star was observed with UVES, and the remaining eight using GIRAFFE. Most of the *CoRoT* Li-rich giant stars are approximately around solar metallicity, with a higher frequency of stars observed just below the RGB bump. However, at least two, perhaps three, stars are consistent with being more evolved.

19301883–0004175 is the coolest and most metal-poor Li-rich star in our sample ($T_{\rm eff} = 4070$ K, [Fe/H] $= -0.52$). In contrast to observations where most Li-rich giant stars are found below the RGB bump, 19301883–0004175 adds to the small sample of Li-rich stars at more evolved stages. Li-rich giant stars past the RGB bump are preferentially more metal-poor, consistent with 19301883–0004175.

Given the stellar parameters, 19230935+0123293 is consistent with being a red clump star. The uncertainties in stellar parameters for 19253819+0031094 are relatively large, therefore its exact evolutionary stage is uncertain. Given the uncertainties in stellar parameters and the tendency of solar-metallicity Li-rich giants to occur more frequently around the RGB bump, it is perhaps likely that 19230935+0123293 is indeed located near the RGB bump, as indicated by the reported stellar parameters. The ambiguity in evolutionary stage for these stars would be easily resolved if astereoseismic oscillations were detectable for these objects. However, at this stage, it would appear these stars are slightly too faint for the evolutionary stage to be derived from *CoRoT* light curves.

[3] http://keplerscience.arc.nasa.gov/

### 3.2 Explaining the Li-rich giant phenomena

Here we discuss the plausibility of internal and external mechanisms proposed to reconcile observed properties of Li-rich giants. We note that our data are inadequate to comment on external mechanisms involving supernovae or transient X-ray binaries, therefore we do not consider this hypothesis further.

The internal scenarios that we have previously outlined describe the deep mixing conditions required to produce an increased surface Li-abundance. However – other than thermohaline mixing – these models lack any description for why a given star begins to experience deep mixing, or why the frequency of stars undergoing deep mixing is so low. Therefore, while the Li production mechanism and the conditions required for it to occur are well-understood, there still exists a *missing link* in exactly what causes the extra mixing.

#### *3.2.1 Are Li-rich K-type giants likely due to planet ingestion?*

The increasing number of stars known to host close-in giant planets ("hot Jupiters") provides a potential solution to the Li-rich giant problem. In this framework two factors actually contribute towards the increase in surface Li abundance: (1) the injection of a large planet provides a reservoir of primordial (unburnt) levels of lithium, and (2) deep mixing that is induced as the planet is dissipated throughout the convective envelope, bringing freshly produced Li to the surface.

Siess & Livio (1999a,b) first explored this scenario theoretically and showed that while the results are sensitive to the accretion rate and structure of the star, the accretion of a planet or brown dwarf star can produce the requisite surface Li abundance and explain their frequency. However, this mechanism was invoked to reconcile the existence of Li-rich giants across the RGB and the AGB, which is not commensurate with the properties of close-in hot Jupiters or their occurrence rates.

Exoplanet occurrence rates are correlated with the host star. For example, close-in giant planets form preferentially around metal-rich stars (e.g., Santos et al. 2004; Fischer & Valenti 2005). Indeed, the frequency of metal-rich giant planets is well-represented as a log-linear function of the host star metallicity (e.g., Fischer & Valenti 2005). For FGK stars with near-solar metallicity, the fraction of stars hosting close-in giant planets is approximately 8%, and decreases to 0.6% for stars of [Fe/H] $= -0.5$ (Schlaufman 2014).

The occurrence rate of close-in giant planets also appears to be a function of the evolutionary state of the host star. It is well-established that sub-giant stars have systematically higher giant planet occurrence rates when all orbital periods are considered. However, sub-giant stars are also found to have fewer close-in hot Jupiters than main-sequence stars of the same metallicity (Bowler et al. 2010; Johnson et al. 2010). There has been considerable debate to explain the differing occurrence rates of close-in hot Jupiters, including suggestions that stellar mass differences between the two populations is sufficient to explain the discrepancy (Burkert & Ida 2007; Pasquini et al. 2007; Kennedy & Kenyon 2008a,b). If the sub-giant stellar masses were considerably larger than those of main-sequence stars at the same metal-

licity, then one could imagine changes in the proto-planetary disk or dissipation timescales (due to increased radiative pressure) that could hamper the formation of close-in giant planets and reconcile the observations (Kennedy & Kenyon 2009). The alternative scenario is that close-in giant planets become tidally destroyed as stars leave the main-sequence and the convective envelope increases. It would be difficult to unambiguously resolve these two possibilities (difference in stellar masses or tidal destruction of hot Jupiters) using models of stellar evolution and planet formation, given the number of unknown variables.

Schlaufman & Winn (2013) employed a novel approach to untangle this mystery using precise Galactic space motions. Their sample comprised main-sequence and sub-giant F- and G-type stars in the thin disk. Thin disk stars form with a very cold velocity distribution because they grow from dense, turbulent gas in a highly dissipative process. Over time the velocity distribution for a thin disk stellar population increases due to interactions between stars, molecular clouds and spiral waves. Because massive stars spend very little time on the main-sequence, there is only a short period for interactions to kinematically heat a population of massive stars. In contrast, solar-mass stars spend a long time on the main-sequence, allowing for plenty of interactions to kinematically heat the population. For these reasons one would expect the space velocity dispersion of thin disk stars to decrease with increasing stellar mass. This logic extends to evolved stars, since they only spend a small fraction as a sub-giant or giant relative to their main-sequence lifetime.

Using precise parallaxes and proper motions from *Hipparcos* (van Leeuwen 2007), Schlaufman & Winn (2013) find that the distribution of Galactic space motions of planet-hosting sub-giant stars are on average equal to those of planet-hosting main-sequence stars. For this reason, the distribution of planet-hosting sub-giant and main-sequence stars can only differ in age (or radius, as expected from the increasing stellar envelope), but not mass. Moreover the orbital eccentricities of Jupiters around sub-giants are systematically lower than those of main-sequence stars (e.g., Jones et al. 2014), indicating that some level of angular momentum transfer and orbital circularisation has occurred. Because the main-sequence and sub-giant planet-host stars are likely to only differ in age, they provide insight on what happens to close-in giant planets when a star's convective envelope deepens at the base of the giant branch. Therefore the lack of close-in giant planets orbiting sub-giant stars provides clear evidence for their destruction (e.g., Rasio & Ford 1996; Villaver & Livio 2009; Lloyd 2011; Schlaufman 2014).

Given this empirical evidence for tidal destruction of close-in hot Jupiters as a star begins its ascent on the giant branch, it is intriguing to consider what impact the planet accretion would have on the host star. Siess & Livio (1999b) show that while the extent of observable signatures are sensitive to the mass of the planet and the accretion rate, the engulfment of a close-in giant planet can significantly increase the photospheric Li abundance. Recall that two factors contribute to this signature. Firstly, the accreted mass of the giant planet – where no Li burning has occurred – can produce a net increase in photospheric Li. The second effect allows for Li *production* within the star: the spiralling infall of a giant planet and the associated angular momentum transfer is sufficient to induce deep mixing, bringing freshly produced $^7$Li to the surface before it is destroyed.

If the additional Li reservoir were the only effect contributing to the net increase in photospheric Li, then an order-of-magnitude estimate of the requisite planetary mass suggests a brown dwarf is required. However a brown dwarf will have a fully convective envelope, and will therefore have depleted some of its primordial Li abundance. Moreover, the lack of brown dwarfs found within 3-5 AU around solar-mass stars (<1%; the *'brown dwarf desert'*, see Grether & Lineweaver 2006) indicates that brown dwarfs are not frequent enough to later produce the higher frequency of Li-rich giant stars. For these reasons Li-rich giant stars are unlikely to be primarily produced from the ingestion of a brown dwarf, implying that the deep mixing induced by angular momentum transfer is crucial to produce high photospheric Li abundances. Moreover, without any additional mixing (and just a reservoir of unburnt Li) we would expect a similar increase in Be, which has not been detected in Li-rich giant stars to date (de Medeiros et al. 1997; Castilho et al. 1999; Melo et al. 2005; Monaco et al. 2014).

Indeed, if we simply take the models of Siess & Livio (1999a,b) at face value and assume that *some* conditions of accretion rate can produce a net increase in photospheric Li (either through a fresh reservoir of Li and induced deep mixing), then the observed occurrence rates of close-in giant planets *predicts a population of Li-rich giant stars before the RGB bump*. The occurrence rates of close-in giant planets at solar metallicity (≈8%, or more conservatively ≈1%, e.g., Santerne et al. 2015) is commensurate with the idea that some accretion conditions could produce a population of Li-rich giant stars with a frequency of ≈1%.

If this scenario were true, the correlation between the occurrence rate of close-in giant planets and the host stellar metallicity suggests that we should expect to see more Li-rich giant stars before the RGB bump with higher metallicities. Although the lack of reproducible selection functions for studies of Li-rich giant stars prevents us from commenting on the fraction of Li-rich giants at a given metallicity, the observations are consistent with our expectations. Indeed, like Martell & Shetrone (2013), we find that most of our Li-rich giant stars have near-solar metallicities. However this observation may be complicated by the *Gaia-ESO Survey* selection function, as the metallicity distribution function of *Gaia-ESO Survey* stars peaks near solar metallicity for the UVES sample in iDR4.

Contrary to the original motivation in Siess & Livio (1999a), the planet engulfment model is actually less likely to produce Li-rich stars all across the RGB and AGB, because close-in giants are likely to be destroyed as soon as the convective envelope increases. Although planets are found more frequently around sub-giant stars, those planets are preferentially found on long orbital periods. Moreover, the timescale of Li-depletion suggests that our proposed scenario is unlikely to account for highly evolved stars with increased Li. As the planet is destroyed the subsequent Li enhancement will be depleted over the next ∼0.2–1 Myr. Because low-mass stars spend such a short time from the main-sequence to the sub-giant phase, we should expect any Li enhancement to be depleted by the time they have ascended even moderately up the giant branch.

Alternatively, if a giant planet is formed sufficiently far

from the host star it may be unaffected by the initial expansion of the convective envelope. In this scenario it may be accreted at a subsequent time, ultimately being destroyed when the star is more evolved. However the circularisation and long orbital periods of giant planets around sub-giant stars suggests that the long-timescale engulfment scenario is somewhat improbable (Jones et al. 2014; Schlaufman 2014). On the other hand, one could imagine a somewhat unusual scenario where the planet is not fully dissolved, and orbits within the stellar photosphere without any large transfer of angular momentum. In principle, this kind of scenario may explain Li-rich giant stars at more evolved stages.

Our assertion linking the majority of Li-rich stars as a consequence of tidal destruction of close-in giant planets is unlikely to fully explain the existence of very metal-poor Li-rich giants. The occurrence rates of close-in giant planets for stars with low metallicity ([Fe/H] $= -0.5$) is a mere $\sim$1%, and decreases with total metallicity. Therefore, a very metal-poor star (e.g., [Fe/H] $< -2$) is quite unlikely to host any planet (including a close-in giant planet), and therefore planet accretion is an improbable explanation for the increased surface Li. However, of the Li-rich stars that are also metal-poor, these are almost ubiquitously found to also be highly evolved (e.g., AGB, RGB tip, red clump), which are thus explainable through a host of internal mechanisms.

Dynamical interactions would suggest that our proposed link between close-in giant planets and Li-rich giants implies a lower fraction of Li-rich giant stars should be found in dense stellar environments. Three body interactions in a dense cluster can sufficiently perturb a close-in hot Jupiter before a star leaves the main-sequence (Sigurdsson 1992; Hurley & Shara 2002). While the evidence is weak, this appears to be consistent with the observations of Li-rich giants (see Section 3.3).

#### *3.2.2 Has the evolutionary stage been mis-estimated?*

An alternative scenario is that spectroscopic studies of Li-rich giants are systematically biased in their determination of surface gravities. Indeed, if the majority of Li-rich giant stars are actually red clump stars that have been misclassified as stars below the bump, there may be little or no requirement for an external mechanism to induce additional mixing.

In their low-resolution study of $\sim 2,000$ low-mass giant stars, Kumar et al. (2011) identified fifteen new Li-rich stars and noted a concentration of them at the red clump, or on the RGB. Either evolutionary state was plausible, as it is difficult to unambiguously determine the precise evolutionary state directly from spectroscopy. Because the lifetime for clump stars is much longer than those at the bump, it is reasonable to expect that many field stars identified to be near the luminosity bump are indeed clump stars. Moreover, stellar evolution models suggest that Li can be synthesised during the He-core flash (Eggleton et al. 2008; Kumar et al. 2011), suggesting that most Li-rich giants may actually be red clump stars, and have been mis-identified as being near the luminosity bump.

Silva Aguirre et al. (2014) used asteroseismic data from the *Kepler* space telescope and came to this conclusion for their metal-poor ([Fe/H] $= -0.29$) Li-rich star. Although stellar parameters derived from spectroscopy alone were unable to confidently place their star on the RGB or at the clump, the internal oscillations for a star with or without a He-burning core show small differences (Bedding et al. 2011; Mosser et al. 2011). However Jofré et al. (2015) showed that solar-like oscillations in KIC 9821622 (another Li-rich giant star) demonstrated that it does not have a He-burning core, and firmly places the evolutionary stage of KIC 9821622 below the luminosity bump on the giant branch.

Our sample constitutes the largest number of Li-rich giant stars identified in a field observed by a space telescope capable of detecting asteroseimic oscillations. Although our stellar parameters are more consistent with the majority of these stars being on the RGB at or below the luminosity bump, they are each *individually* consistent with being red clump stars: the red clump position (in $T_{\rm eff}$ and $\log g$) is 1-$\sigma$ to 2-$\sigma$ of the quoted uncertainty for each *individual* star. However as a coherent sample, the *population* significance depends on how correlated these measurements are. For these reasons, employing asteroseismic data from *CoRoT* may reveal whether these stars are indeed red clump stars, or associated with the bump in the luminosity. If indeed it is the former, an external planet ingestion scenario becomes unlikely, which would provide strong direction on where to focus modelling efforts. We encourage follow-up work to distinguish these possibilities.

### 3.3 Frequency of Li-rich K giants

The selection function and observing strategy employed for the *Gaia-ESO Survey* preclude us from robustly commenting on the frequency of Li-rich giants for the Milky Way field population. All UVES spectra include the 6707 Å Li line, but the standard GIRAFFE settings used for Milky Way *Survey* fields (HR10 and HR21) do not span this region. *CoRoT* observations within the *Gaia-ESO Survey* are a unique subset of high scientific interest, which is why the HR15N setup (covering Li) was employed for these stars. Therefore we can only comment on the frequency of Li-enhanced (A(Li) $\gtrsim 2$) K-giant stars identified in the *CoRoT* field, or the fraction observed in the larger UVES sample.

At first glance the discovery of 9 Li-rich giant stars in the *CoRoT* field may appear as a statistically high number, suggesting there may be something special about the location of the *CoRoT* field, or the distribution of stellar masses within it. The *Gaia-ESO Survey* iDR4 contains 1,175 giant stars that match our selection criteria ($\log g < 3$ and $T_{\rm eff} < 5200$ K) where the abundance of Li is reported. We identify 9 Li-rich giants, resulting in an observed frequency of slow rotating Li-rich K giants of $\sim$1%, consistent with previous studies (e.g., Drake et al. 2002).

The frequency in the total UVES sample from the *Gaia-ESO Survey* iDR4 is even smaller. The sample contains 992 giants that match our selection criteria, of which 845 have Li abundance measurements or upper limits. Four of these are Li-rich, implying a frequency of just 0.4%. These are small-number statistics that may be strongly impacted by the *Survey* selection function. For example, the UVES sample contains a considerable fraction (27%) of cluster stars. Only about 50% of the sample are Milky Way fields, with the remainder comprised of bulge fields, benchmark stars, and radial velocity standards. The UVES cluster sample (open and globular) contains 256 stars, of which two are Li-rich.

It is of interest to speculate whether the occurrence rate of slow-rotating Li-rich K giants differs between clusters and the field. While it is difficult for us to make robust inferences on the field frequency based on the literature or the iDR4 *Survey* data set, it is important to note that the vast majority ($\gtrsim 90\%$) of Li-rich giant stars *have* been discovered in the field. After accounting for the fact that star clusters have been extensively observed with multi-object spectroscopic instruments for over a decade, it seems curious that less than ten Li-rich giant stars have been detected in globular clusters to date. However, we stress that standard instrumental setups do not always include the Li line, so this line of argument is further complicated by observational (or scientific) biases.

## 4 CONCLUSIONS

We have presented one of the largest samples of Li-rich K-giant stars. Our sample of Li-rich giant stars includes the most Li-rich giant known towards the bulge, and the first sample of Li-rich giants towards the *CoRoT* fields. Most stars have stellar parameters and abundances that are consistent with being just below the luminosity bump on the red giant branch. Given that about half of our sample is towards the *CoRoT* fields, accurately knowing the evolutionary stage of this sample could confirm their position below the luminosity bump.

The ensemble properties of Li-rich giant stars in the literature suggest two sub-classes, which may point towards their formation mechanism(s). The first is comprised of near-solar ($[\mathrm{Fe/H}] \gtrsim -0.5$) metallicity stars, which are preferentially found slightly before or near the luminosity bump. The second class of Li-rich giants are found in later evolutionary stages and are usually more metal-poor.

We argue that Li-rich giant stars before or near the luminosity bump are a consequence of planet/brown dwarf engulfment when the stellar photosphere expands at the sub-giant stage. Our assertion is supported by recent evidence on the occurrence rates of close-in giant planets, which demonstrate that hot Jupiters are accreted onto the host star as they begin to ascend the giant branch. If we take planet accretion models at face value and trust that *some* conditions of accretion rate can produce a net positive abundance of Li by amassing unburnt Li *and* inducing deep mixing by angular momentum transfer, then these two lines of evidence actually *predict the existence of Li-rich giant stars*.

This scenario would predict an increasing frequency of Li-rich giant stars with increasing metallicity, and the Li-depletion timescales would suggest that these stars should be preferentially found below the RGB bump. Moreover, it would imply a lower fraction of Li-rich giant stars in dense stellar environments (e.g., clusters) due to three body interactions. The majority of Li-rich giant stars are consistent with these predictions. The remainder are mostly Li-rich giant stars at late evolutionary stages, a fact that is reconcilable with internal mixing prescriptions, late-time engulfment, or mass-transfer from a binary companion.

## ACKNOWLEDGMENTS

We thank the anonymous referee for a constructive report which improved this paper. We thank Ross Church, Ghina Halabi, Jarrod Hurley, Benoit Mosser, Kevin Schlaufman, as well as the *Gaia/Stars* and *Stellar Interiors* research groups at the Institute of Astronomy, University of Cambridge for helpful discussions on this work. Based on data products from observations made with ESO Telescopes at the La Silla Paranal Observatory under programme ID 188.B-3002. These data products have been processed by the Cambridge Astronomy Survey Unit (CASU) at the Institute of Astronomy, University of Cambridge, and by the FLAMES/UVES reduction team at INAF/Osservatorio Astrofisico di Arcetri. These data have been obtained from the Gaia-ESO Survey Data Archive, prepared and hosted by the Wide Field Astronomy Unit, Institute for Astronomy, University of Edinburgh, which is funded by the UK Science and Technology Facilities Council. This work was partly supported by the European Union FP7 programme through ERC grant number 320360 and by the Leverhulme Trust through grant RPG-2012-541. We acknowledge the support from INAF and the Ministero dell Istruzione, dell Universita e della Ricerca (MIUR) in the form of the grant Premiale VLT 2012 and The Chemical and Dynamical Evolution of the Milky Way and Local Group Galaxies (prot. 2010LY5N2T). The results presented here benefit from discussions held during the Gaia-ESO workshops and conferences supported by the ESF (European Science Foundation) through the GREAT Research Network Programme. G. R. acknowledges support from the project grant "The New Milky Way" from the Knut and Alice Wallenberg Foundation. G. M. K is supported by the Royal Society as a Royal Society University Research Fellow. L. S. acknowledges support provided by the Chilean Ministry of Economy, Development, and Tourisms Millennium Science Initiative through grant IC120009, awarded to The Millennium Institute of Astrophysics, MAS. Funding for the Stellar Astrophysics Centre is provided by The Danish National Research Foundation. The research is supported by the ASTERISK project (ASTERoseismic Investigations with SONG and Kepler) funded by the European Research Council (Grant agreement no.: 267864). V. S. A. acknowledges support from VILLUM FONDEN (research grant 10118). S. L. M acknowledges support from the Australian Research Council through DECRA fellowship DE140100598. T. M. acknowledges financial support from Belspo for contract PRODEX *Gaia*-DPAC. J. M. acknowledges the support from the European Research Council Consolidator Grant funding scheme (*project STARKEY*, G.A. n. 615604). This research has made use of the ExoDat Database, operated at LAM-OAMP, Marseille, France, on behalf of the CoRoT/Exoplanet program. This research made use of Astropy, a community-developed core Python package for Astronomy (Astropy Collaboration et al. 2013). This research has made use of NASA's Astrophysics Data System Bibliographic Services.

## REFERENCES

Adamów, M., Niedzielski, A., Villaver, E., Wolszczan, A., & Nowak, G. 2014, A&A, 569, A55

Adamów, M., Niedzielski, A., Villaver, E., et al. 2015, A&A, 581, A94
Alcalá, J. M., Biazzo, K., Covino, E., Frasca, A., & Bedin, L. R. 2011, A&A, 531, L12
Alexander, J. B. 1967, The Observatory, 87, 238
Andrievsky, S. M., Gorlova, N. I., Klochkova, V. G., Kovtyukh, V. V., & Panchuk, V. E. 1999, Astronomische Nachrichten, 320, 35
Anthony-Twarog, B. J., Deliyannis, C. P., Rich, E., & Twarog, B. A. 2013, ApJ, 767, L19
Astropy Collaboration, Robitaille, T. P., Tollerud, E. J., et al. 2013, Astronomy & Astrophysics, 558, AA33
Balachandran, S. C., Fekel, F. C., Henry, G. W., & Uitenbroek, H. 2000, ApJ, 542, 978
Barrado y Navascues, D., de Castro, E., Fernandez-Figueroa, M. J., Cornide, M., & Garcia Lopez, R. J. 1998, A&A, 337, 739
Bedding, T. R., Mosser, B., Huber, D., et al. 2011, Nature, 471, 608
Bensby, T., Yee, J. C., Feltzing, S., et al. 2013, A&A, 549, A147
Bonsack, W. K. 1959, ApJ, 130, 843
Bowler, B. P., Johnson, J. A., Marcy, G. W., et al. 2010, ApJ, 709, 396
Bressan, A., Marigo, P., Girardi, L., et al. 2012, MNRAS, 427, 127
Brown, J. A., Sneden, C., Lambert, D. L., & Dutchover, E., Jr. 1989, ApJS, 71, 293
Burkert, A., & Ida, S. 2007, ApJ, 660, 845
Cameron, A. G. W., & Fowler, W. A. 1971, ApJ, 164, 111
Canto Martins, B. L., Lèbre, A., de Laverny, P., et al. 2006, A&A, 451, 993
Carlberg, J. K., Smith, V. V., Cunha, K., Majewski, S. R., & Rood, R. T. 2010, ApJ, 723, L103
Carlberg, J. K., Smith, V. V., Cunha, K., et al. 2015, ApJ, 802, 7
Carney, B. W., Fry, A. M., & Gonzalez, G. 1998, AJ, 116, 2984
Casey, A. R., et al. 2016, in preparation
Cassisi, S., Salaris, M., & Pietrinferni, A. 2016, A&A, 585, A124
Castilho, B. V., Spite, F., Barbuy, B., et al. 1999, A&A, 345, 249
Chanamé, J., Pinsonneault, M., & Terndrup, D. M. 2005, ApJ, 631, 540
Charbonnel, C. 1994, A&A, 282, 811
Charbonnel, C. 1995, ApJ, 453, L41
Charbonnel, C., & Balachandran, S. C. 2000, A&A, 359, 563
Charbonnel, C. 2006, EAS Publications Series, 19, 125
Charbonnel, C., & Lagarde, N. 2010, A&A, 522, A10
Charbonnel, C., & Zahn, J.-P. 2007, A&A, 467, L15
Cottrell, P. L., & Da Costa, G. S. 1981, ApJ, 245, L79
Damiani, F., Prisinzano, L., Micela, G., et al. 2014, A&A, 566, A50
da Silva, L., Girardi, L., Pasquini, L., et al. 2006, A&A, 458, 609
Delgado Mena, E., Tsantaki, M., Sousa, S. G., et al. 2015, arXiv:1512.05296
Dias, W. S., Monteiro, H., Caetano, T. C., et al. 2014, A&A, 564, A79
Denissenkov, P. A., & Herwig, F. 2004, ApJ, 612, 1081
Denissenkov, P. A., & VandenBerg, D. A. 2003, ApJ, 593, 509
Denissenkov, P. A., & Weiss, A. 2000, A&A, 358, L49
de La Reza, R., Drake, N. A., & da Silva, L. 1996, ApJ, 456, L115
de La Reza, R., Drake, N. A., da Silva, L., Torres, C. A. O., & Martin, E. L. 1997, ApJ, 482, L77
de la Reza, R., Drake, N. A., Oliveira, I., & Rengaswamy, S. 2015, ApJ, 806, 86
de Medeiros, J. R., Lebre, A., de Garcia Maia, M. R., & Monier, R. 1997, A&A, 321, L37
Dekker, H., D'Odorico, S., Kaufer, A., Delabre, B., & Kotzlowski, H. 2000, Proceedings of SPIE, 4008, 534
D'Orazi, V., Gratton, R. G., Angelou, G. C., et al. 2015, ApJ, 801, L32
Drake, N. A., de la Reza, R., da Silva, L., & Lambert, D. L. 2002, AJ, 123, 2703
Eggleton, P. P., Dearborn, D. S. P., & Lattanzio, J. C. 2006, Science, 314, 1580
Eggleton, P. P., Dearborn, D. S. P., & Lattanzio, J. C. 2008, ApJ, 677, 581
Fekel, F. C., & Balachandran, S. 1993, ApJ, 403, 708
Fekel, F. C., & Watson, L. C. 1998, AJ, 116, 2466
Fischer, D. A., & Valenti, J. 2005, ApJ, 622, 1102
Fulbright, J. P., McWilliam, A., & Rich, R. M. 2007, ApJ, 661, 1152
Gilmore, G., Randich, S., Asplund, M., et al. 2012, The Messenger, 147, 25
Gonzalez, O. A., Zoccali, M., Monaco, L., et al. 2009, A&A, 508, 289
Gratton, R. G., & D'Antona, F. 1989, A&A, 215, 66
Gratton, R. G., Sneden, C., Carretta, E., & Bragaglia, A. 2000, A&A, 354, 169
Grether, D., & Lineweaver, C. H. 2006, ApJ, 640, 1051
Grevesse, N., Asplund, M., & Sauval, A. J. 2007, Space Sci.Rev., 130, 105
Gustafsson, B., Edvardsson, B., Eriksson, K., et al. 2008, A&A, 486, 951
Hanni, L. 1984, Soviet Astronomy Letters, 10, 51
Heiter, U., Lind, K., Asplund, M., et al. 2015, Physica Scripta, 90, 054010
Hill, V., & Pasquini, L. 1999, A&A, 348, L21
Hurley, J. R., & Shara, M. M. 2002, ApJ, 565, 1251
Iben, I., Jr. 1964, ApJ, 140, 1631
Iben, I., Jr. 1967, ApJ, 147, 624
Iben, I., Jr. 1967, ApJ, 147, 650
Janes, K. A., & Hoq, S. 2011, AJ, 141, 92
Jasniewicz, G., Parthasarathy, M., de Laverny, P., & Thévenin, F. 1999, A&A, 342, 831
Jofré, E., Petrucci, R., García, L., & Gómez, M. 2015, A&A, 584, L3
Johnson, J. A., Howard, A. W., Bowler, B. P., et al. 2010, PASP, 122, 701
Jones, M. I., Jenkins, J. S., Bluhm, P., Rojo, P., & Melo, C. H. F. 2014, A&A, 566, A113
Karakas, A. I. 2010, MNRAS, 403, 1413
Karakas, A. I., & Lattanzio, J. C. 2014, PASA, 31, e030
Kennedy, G. M., & Kenyon, S. J. 2008, ApJ, 673, 502
Kennedy, G. M., & Kenyon, S. J. 2008, ApJ, 682, 1264
Kennedy, G. M., & Kenyon, S. J. 2009, ApJ, 695, 1210
Kirby, E. N., Fu, X., Guhathakurta, P., & Deng, L. 2012, ApJ, 752, L16

Kirby, E. N., Guhathakurta, P., Zhang, A. J., et al. 2016, arXiv:1601.01315
Kővári, Z., Korhonen, H., Strassmeier, K. G., et al. 2013, A&A, 551, A2
Kraft, R. P., Peterson, R. C., Guhathakurta, P., et al. 1999, ApJ, 518, L53
Kumar, Y. B., Reddy, B. E., & Lambert, D. L. 2011, ApJ, 730, L12
Kumar, Y. B., Reddy, B. E., Muthumariappan, C., & Zhao, G. 2015, A&A, 577, A10
Lagarde, N., Decressin, T., Charbonnel, C., et al. 2012, A&A, 543, A108
Lambert, D. L., Dominy, J. F., & Sivertsen, S. 1980, ApJ, 235, 114
Lanzafame, A. C., Frasca, A., Damiani, F., et al. 2015, A&A, 576, A80
Lattanzio, J. C., Siess, L., Church, R. P., et al. 2015, MNRAS, 446, 2673
Lèbre, A., de Laverny, P., Do Nascimento, J. D., Jr., & de Medeiros, J. R. 2006, A&A, 450, 1173
Lèbre, A., Palacios, A., Do Nascimento, J. D., Jr., et al. 2009, A&A, 504, 1011
Lewis, J, et al. 2016, in preparation
Lind, K., Asplund, M., & Barklem, P. S. 2009, A&A, 503, 541
Lind, K., Primas, F., Charbonnel, C., Grundahl, F., & Asplund, M. 2009, A&A, 503, 545
Liu, Y. J., Tan, K. F., Wang, L., et al. 2014, ApJ, 785, 94
Lloyd, J. P. 2011, ApJ, 739, L49
Luck, R. E. 1982, PASP, 94, 811
Martell, S. L., & Shetrone, M. D. 2013, MNRAS,430, 611
Martin, E. L., Rebolo, R., Casares, J., & Charles, P. A. 1992, Nature, 358, 129
Martin, E. L., Rebolo, R., Casares, J., & Charles, P. A. 1994, ApJ, 435, 791
Melo, C. H. F., de Laverny, P., Santos, N. C., et al. 2005, A&A, 439, 227
Mészáros, S., Avrett, E. H., & Dupree, A. K. 2009, AJ, 138, 615
Mosser, B., Barban, C., Montalbán, J., et al. 2011, A&A, 532, A86
Mucciarelli, A., Salaris, M., & Bonifacio, P. 2012, MNRAS, 419, 2195
McWilliam, A., & Rich, R. M. 1994, ApJS, 91, 749
Monaco, L., Villanova, S., Moni Bidin, C., et al. 2011, A&A, 529, A90
Monaco, L., Boffin, H. M. J., Bonifacio, P., et al. 2014, A&A, 564, L6
Ness, M., Freeman, K., Athanassoula, E., et al. 2013, MNRAS, 430, 836
Netopil, M., Paunzen, E., Maitzen, H. M., et al. 2007, A&A, 462, 591
Palacios, A., Charbonnel, C., & Forestini, M. 2001, A&A, 375, L9
Palacios, A., Charbonnel, C., Talon, S., & Siess, L. 2006, A&A, 453, 261
Pasquini, L., Avila, G., Allaert, E., et al. 2000, Proceedings of SPIE, 4008, 129
Pasquini, L., Döllinger, M. P., Weiss, A., et al. 2007, A&A, 473, 979
Pilachowski, C. 1986, ApJ, 300, 289
Randich, S., Gilmore, G., & Gaia-ESO Consortium 2013, The Messenger, 154, 47
Rasio, F. A., & Ford, E. B. 1996, Science, 274, 954
Rebull, L. M., Carlberg, J. K., Gibbs, J. C., et al. 2015, AJ, 150, 123
Reyniers, M., & Van Winckel, H. 2001, A&A, 365, 465
Ruchti, G. R., Fulbright, J. P., Wyse, R. F. G., et al. 2011, ApJ, 743, 107
Ruffoni, M. P., Den Hartog, E. A., Lawler, J. E., et al. 2014, MNRAS, 441, 3127
Sacco, G. G., Morbidelli, L., Franciosini, E., et al. 2014, A&A, 565, A113
Sackmann, I.-J., & Boothroyd, A. I. 1999, ApJ, 510, 217
Santerne, A., Moutou, C., Tsantaki, M., et al. 2015, arXiv:1511.00643
Santos, N. C., Israelian, G., & Mayor, M. 2004, A&A, 415, 1153
Schlaufman, K. C., & Winn, J. N. 2013, ApJ, 772, 143
Schlaufman, K. C. 2014, ApJ, 790, 91
Siess, L., & Livio, M. 1999, MNRAS, 304, 925
Siess, L., & Livio, M. 1999, MNRAS, 308, 1133
Sigurdsson, S. 1992, ApJ, 399, L95
Silva Aguirre, V., Ruchti, G. R., Hekker, S., et al. 2014, ApJ, 784, L16
Skrutskie, M. F., Cutri, R. M., Stiening, R., et al. 2006, AJ, 131, 1163
Smiljanic, R., Korn, A. J., Bergemann, M., et al. 2014, A&A, 570, A122
Smith, V. V., Shetrone, M. D., & Keane, M. J. 1999, ApJ, 516, L73
Spite, F., & Spite, M. 1982, A&A, 115, 357
Sweigart, A. V., & Mengel, J. G. 1979, ApJ, 229, 624
Tajitsu, A., Sadakane, K., Naito, H., Arai, A., & Aoki, W. 2015, Nature, 518, 381
Tautvaišienė, G., Barisevičius, G., Chorniy, Y., Ilyin, I., & Puzeras, E. 2013, MNRAS, 430, 621
Uttenthaler, S., Lebzelter, T., Palmerini, S., et al. 2007, A&A, 471, L41
van Leeuwen, F. 2007, A&A, 474, 653
Villaver, E., & Livio, M. 2009, ApJ, 705, L81
Walker, T. P., Viola, V. E., & Mathews, G. J. 1985, ApJ, 299, 745
Wallerstein, G., & Sneden, C. 1982, ApJ, 255, 577
Wright, E. L., Eisenhardt, P. R. M., Mainzer, A. K., et al. 2010, AJ, 140, 1868

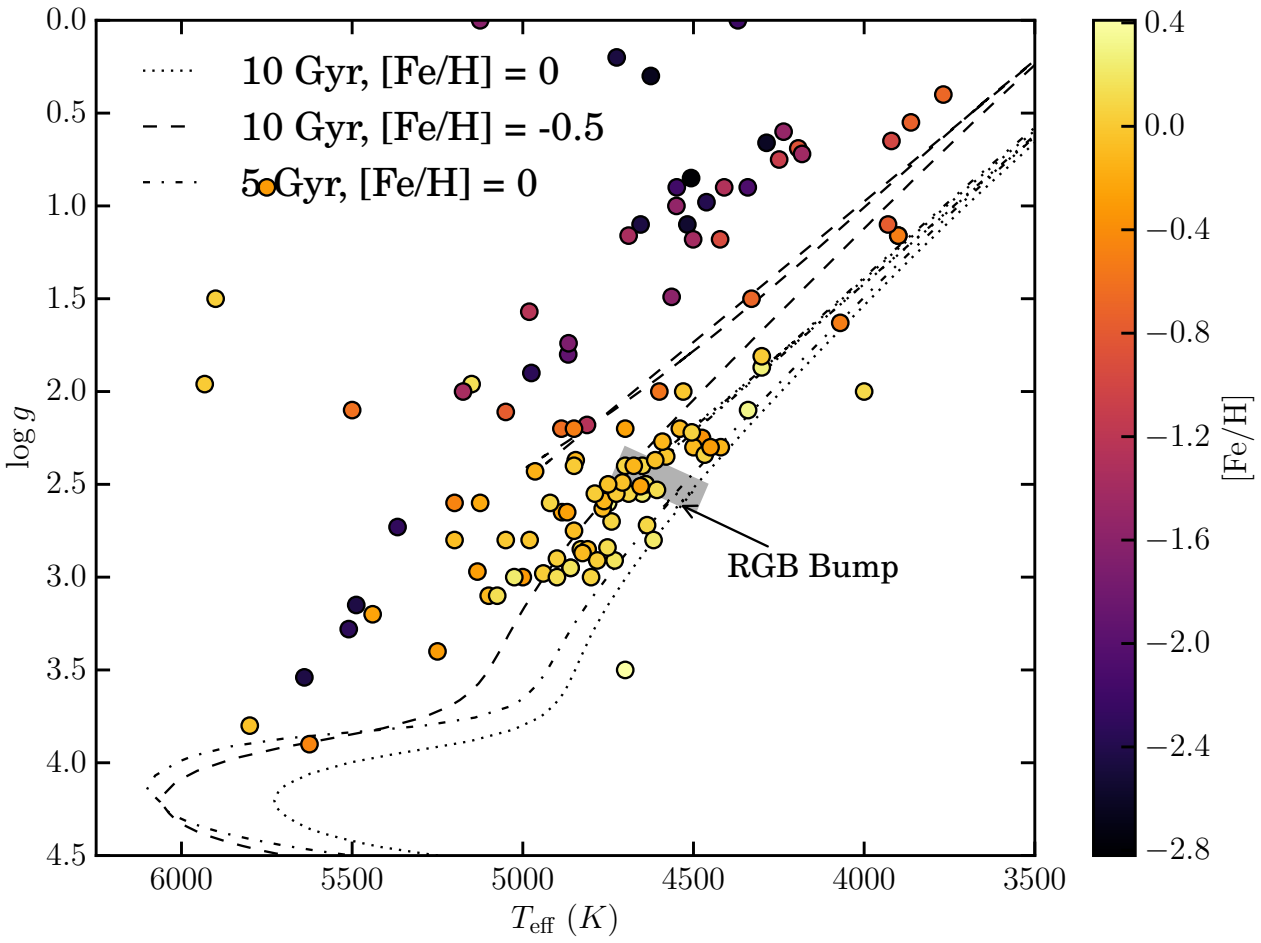


**Figure 1.** Stellar parameters ($T_{\rm eff}$, $\log g$, [Fe/H]) for all 127 giant stars in the literature with A(Li) $> 2$ (in LTE or non-LTE). Discoveries in this study are included. Two 10 Gyr PARSEC isochrones (Bressan et al. 2012, assuming $Z$ is directly proportional to Fe and the PARSEC default $Y = 0.2485 + 1.78Z$) of different metallicity are also shown. Subject to selection functions, this figure indicates that Li-rich giant stars occur more frequently before the luminosity bump on the giant branch, and at near-solar metallicities.

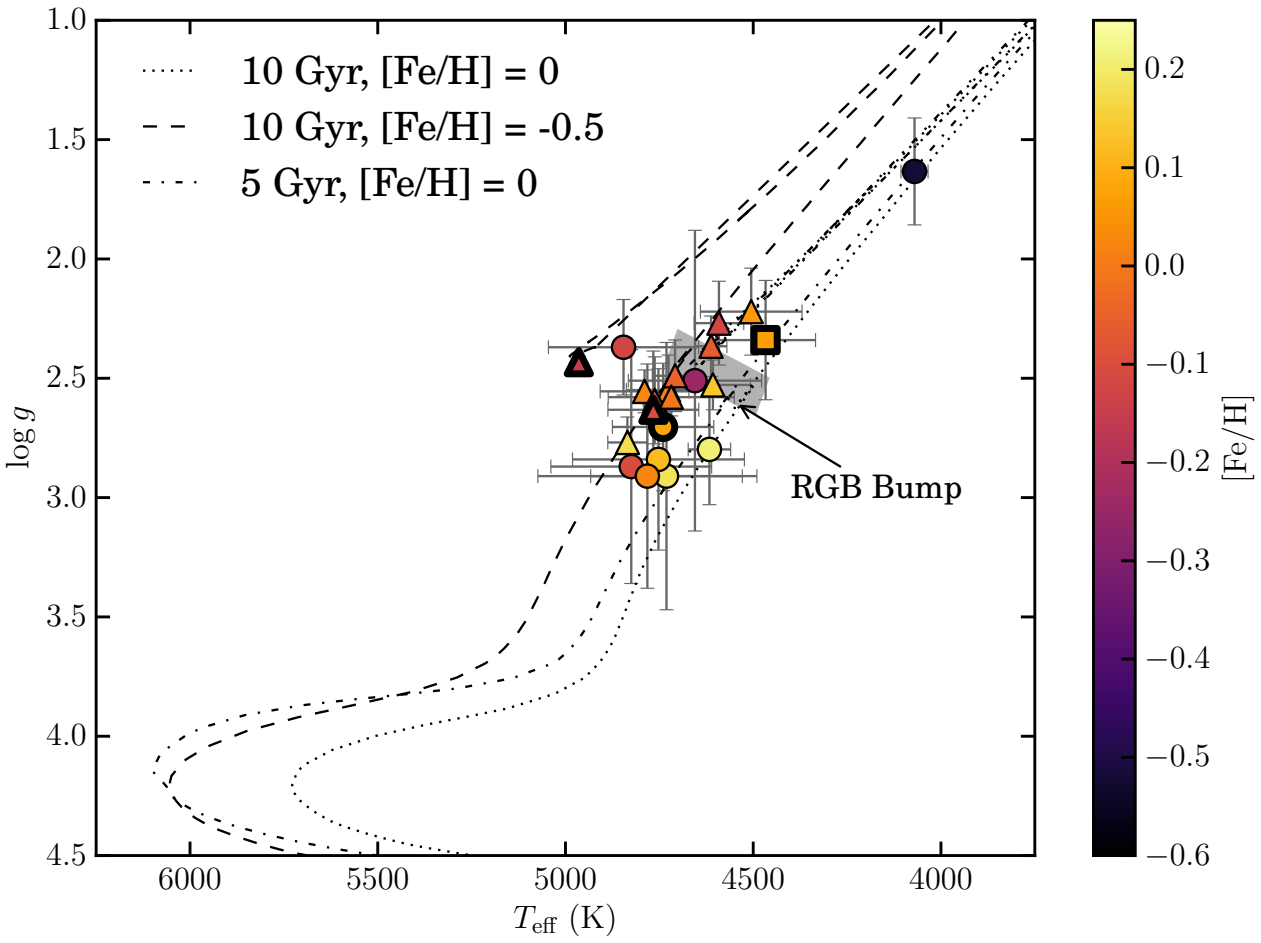


**Figure 2.** Stellar parameters ($T_{\rm eff}$, $\log g$, [Fe/H]) for all Li-rich giant stars in our sample, shown upon 5 Gyr and 10 Gyr PARSEC isochrones with $Y = 0.2485 + 1.78Z$ (Bressan et al. 2012). We highlight the approximate location of the RGB bump from the isochrones shown. Markers are coloured by their metallicity. Thick edges indicate the star was observed with UVES. The bulge Li-rich star is indicated by a square marker, and circular markers indicate *CoRoT* targets.

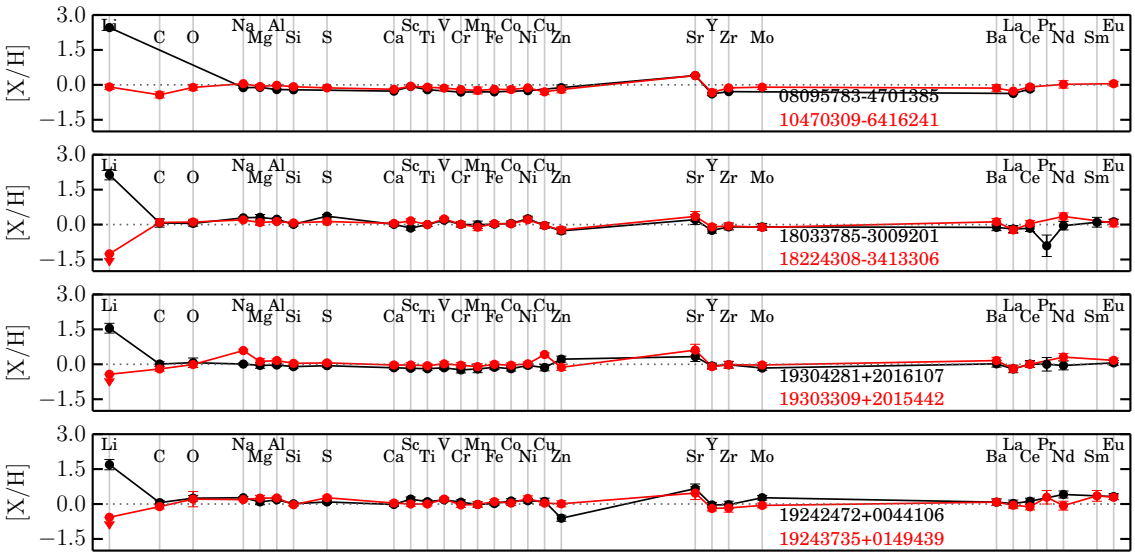


**Figure 3.** Detailed chemical abundances for the 4 Li-rich giant stars identified in the UVES sample of the *Gaia-ESO Survey* iDR4. The detailed chemical abundances of a comparison Li-normal/poor star of similar stellar parameters is shown in red for each Li-rich giant.

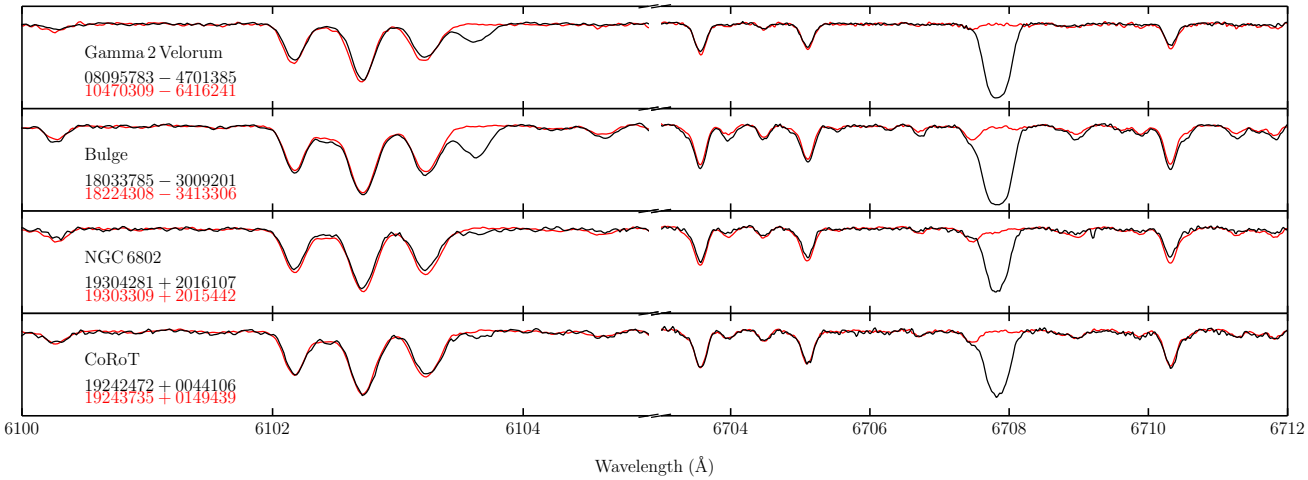


**Figure 4.** Normalised UVES spectra of the 4 Li-rich stars identified in the *Gaia-ESO Survey* iDR4 sample (black), and a comparison star (red) with similar stellar parameters. The resonance Li line at 6707 Å and subordinate line at 6103 Å are visible, clearly showing Li enrichment.

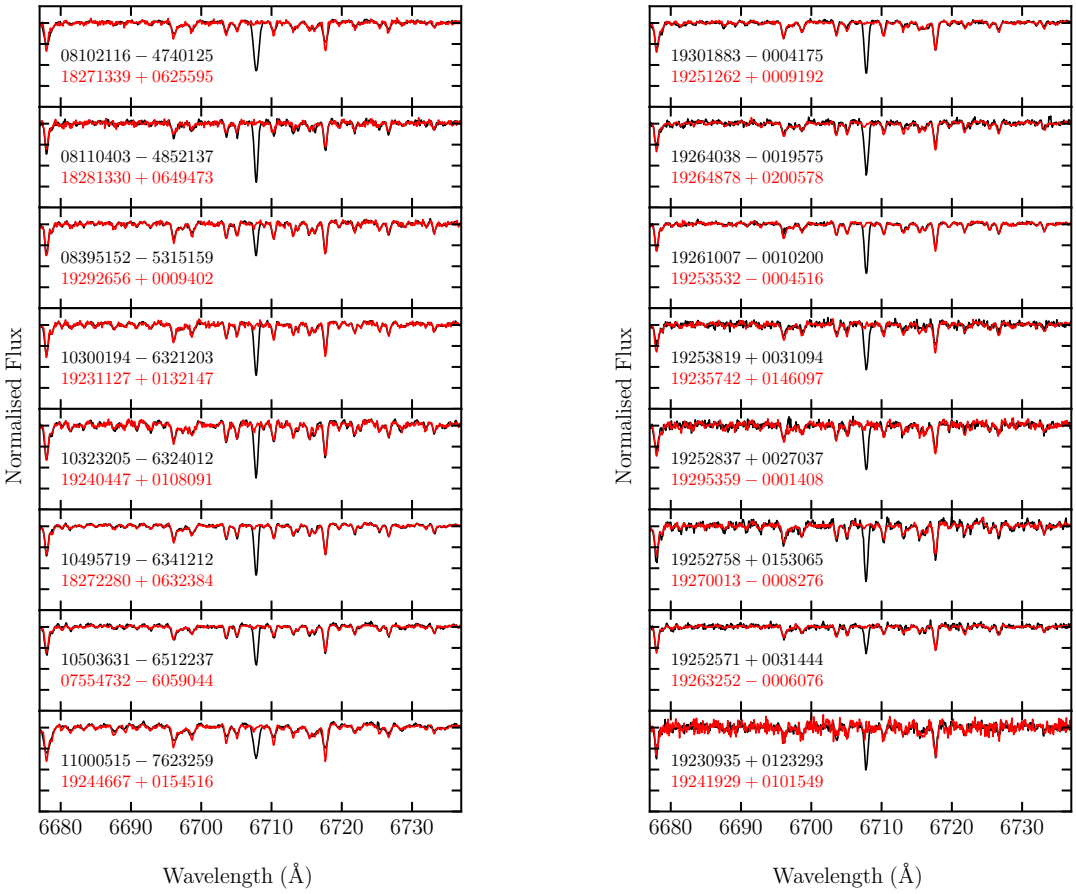


**Figure 4.** Normalised spectra of the Li-rich giant stars observed using GIRAFFE. The resonance Li line at 6707 Å is shown. Spectra for a Li-normal comparison star with similar stellar parameters is shown for each Li-rich giant (red).

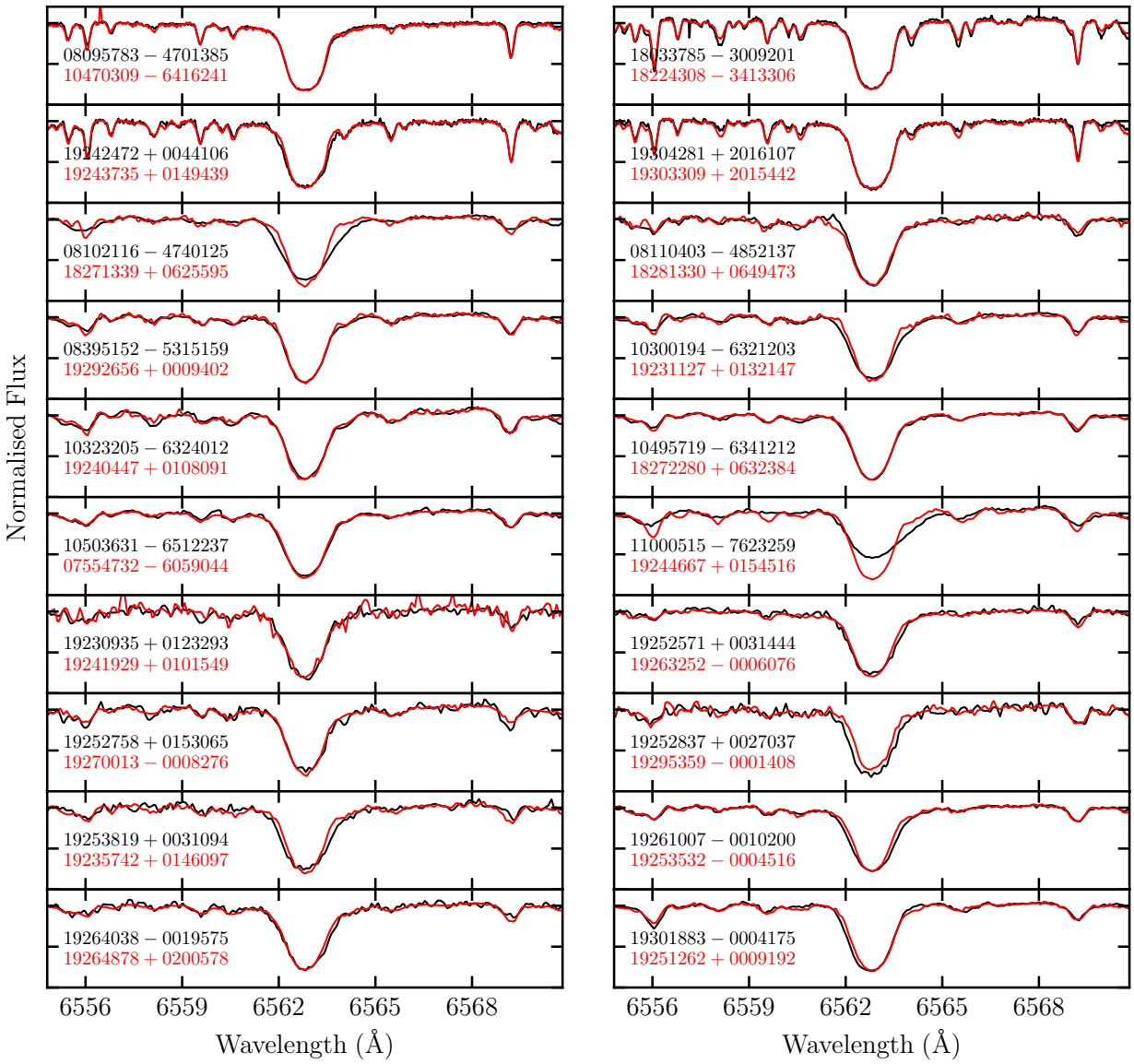


**Figure 5.** A portion of normalised rest-frame spectra for all Li-rich giant stars (black), centered on the H-$\alpha$ line. The UVES stars are shown in the top four panels. If our Li-rich giant stars are experiencing mass-loss through gas, it may be apparent in asymmetries or shifts of H-$\alpha$. A comparison Li-normal/poor star is shown in red for each Li-rich giant.

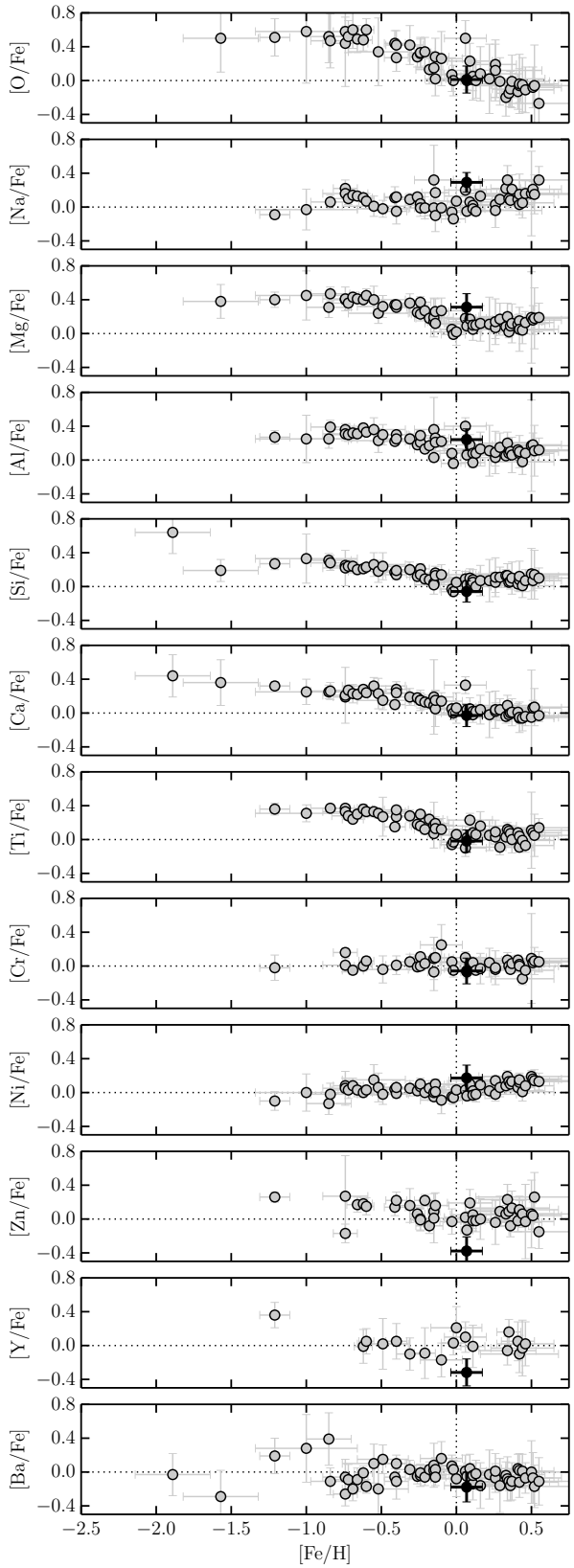


**Figure 6.** Detailed chemical abundances of the Li-rich bulge star, 18033785−3009201, compared to the microlensed bulge dwarf and sub-giant sample of Bensby et al. (2013). The uncertainty in a given [X/Fe] abundance ratio for 18033785−3009201 is taken as the quadrature sum of [X/H] and [X/Fe].

| | Object | $T_{\rm eff}$ | $\log g$ | [Fe/H] | A(Li) | $v \sin i$ | Year | Reference |
|---|---|---|---|---|---|---|---|---|
| 1 | HD172365 | 5500 | 2.1 | -0.6 | 2.49 | 70 | 1982 | Luck (1982) |
| 2 | HD 174104 | 5750 | 0.9 | -0.3 | 3.46 | 50 | 1982 | Luck (1982) |
| 3 | HD 112127 | 4750 | 2.6 | 0.3 | 3.2 | ··· | 1982 | Wallerstein & Sneden (1982) |
| 4 | 9 Bootis (BS 5247) | 4000 | 2.0 | 0.1 | 2.5 | ··· | 1984 | Hanni (1984) |
| 5 | NGC7789-443 | 5600 | 3.1 | ··· | 2.4 | 44 | 1986 | Pilachowski (1986) |
| 6 | NGC7789-1238 | 5800 | 3.1 | ··· | 2.4 | <10 | 1986 | Pilachowski (1986) |
| 7 | NGC7789-308 | 6350 | 3.3 | ··· | 3.0 | 80 | 1986 | Pilachowski (1986) |
| 8 | NGC7789-268 | 6450 | 3.4 | ··· | 3.3 | 30 | 1986 | Pilachowski (1986) |
| 9 | HD 183492 | 4700 | 2.4 | 0.08 | 2.0 | ··· | 1989 | Brown et al. (1989) |
| 10 | HD 126868 | 5440 | 3.2 | -0.25 | 2.3 | ··· | 1989 | Brown et al. (1989) |
| 11 | HD 112127 | 4340 | 2.1 | 0.31 | 2.7 | ··· | 1989 | Brown et al. (1989) |
| 12 | HD 108471 | 4980 | 2.8 | -0.02 | 2.0 | ··· | 1989 | Brown et al. (1989) |
| 13 | HD 148293 | 4640 | 2.5 | 0.23 | 2.0 | ··· | 1989 | Brown et al. (1989) |
| 14 | HD 9746 | 4420 | 2.3 | -0.13 | 2.7 | ··· | 1989 | Brown et al. (1989) |
| 15 | HD 39853 | 3900 | 1.16 | -0.5 | 2.8 | ··· | 1989 | Gratton & D'Antona (1989) |
| 16 | Be21-T33 | 4600 | 2.0 | -0.58 | 3.0 | ··· | 1999 | Hill & Pasquini (1999) |
| 17 | HD 219025 | 4500 | 2.3 | -0.1 | 3.0 | 23 | 1999 | Jasniewicz et al. (1999) |
| 18 | HDE 233517 | 4475 | 2.25 | -0.37 | 3.85 | 17.6 | 2000 | Balachandran et al. (2000) |
| 19 | HD 9746[a] | 4400 | 2.3 | ··· | 3.44 | 9 | 2000 | Balachandran et al. (2000) |
| 20 | HD 172481 | 7250 | 1.5 | -0.55 | 3.57 | 14 | 2001 | Reyniers & Van Winckel (2001) |

**Table 1.** Reported parameters of all known Li-rich giant stars. Only a portion of the table is shown here. The full compilation is available in the online journal. **Before acceptance, full data available at:** https://docs.google.com/spreadsheets/d/1fiHZXyQrGXJivZJh8GCdwc2Zf7wepsTUHBR8BiDfwaI/edit?usp=sharing

| Star | Field | $\alpha$ (J2000) | $\delta$ (J2000) | $J$ | $K$ | $V_{rad}$ (km s$^{-1}$) | $T_{\rm eff}$ (K) | $\log g$ | [Fe/H] |
|---|---|---|---|---|---|---|---|---|---|
| 08095783−4701385 | $\gamma$2 Velorum | 08:09:57.83 | −47:01:38.5 | 10.5 | 9.8 | $25.6 \pm 0.2$ | 4964 | 2.43 | −0.15 |
| 18033785−3009201 | Bulge | 18:03:37.85 | −30:09:20.1 | 11.4 | 10.6 | $-70.0 \pm 0.6$ | 4467 | 2.34 | 0.07 |
| 19242472+0044106 | *CoRoT* | 19:24:24.73 | +00:44:10.5 | 11.3 | 10.5 | $77.7 \pm 0.1$ | 4740 | 2.70 | 0.08 |
| 19304281+2016107 | NGC 6802 | 19:30:42.81 | +20:16:10.7 | 11.7 | 10.7 | $17.4 \pm 0.6$ | 4766 | 2.63 | −0.10 |
| 08102116−4740125 | $\gamma$2 Velorum | 08:10:21.16 | −47:40:12.5 | 11.5 | 10.6 | $71.0 \pm 0.2$ | 4591 | 2.27 | −0.12 |
| 08110403−4852137 | NGC 2547 | 08:11:04.03 | −48:52:13.7 | 12.4 | 11.6 | $54.1 \pm 0.2$ | 4762 | 2.59 | −0.12 |
| 08395152−5315159 | IC2391 | 08:39:51.52 | −53:15:15.9 | 12.4 | 11.5 | $27.0 \pm 0.2$ | 4726 | 2.55 | 0.01 |
| 10300194−6321203 | IC2602 | 10:30:01.94 | −63:21:20.3 | 11.4 | 10.6 | $-10.2 \pm 0.2$ | 4612 | 2.37 | −0.06 |
| 10323205−6324012 | IC2602 | 10:32:32.05 | −63:24:01.2 | 11.3 | 10.6 | $13.3 \pm 0.2$ | 4607 | 2.53 | 0.13 |
| 10495719−6341212 | IC2602 | 10:49:57.19 | −63:41:21.2 | 11.1 | 10.3 | $13.8 \pm 0.2$ | 4789 | 2.55 | 0.03 |
| 10503631−6512237 | IC2602 | 10:50:36.31 | −65:12:23.7 | 11.7 | 10.8 | $-34.1 \pm 0.2$ | 4708 | 2.49 | −0.05 |
| 11000515−7623259 | Chameleon 1 | 11:00:05.15 | −76:23:25.9 | 10.1 | 9.1 | $-15.9 \pm 0.2$ | 4505 | 2.22 | 0.06 |
| 19230935+0123293 | *CoRoT* | 19:23:09.35 | +01:23:29.3 | 13.1 | 12.3 | $11.9 \pm 0.2$ | 4845 | 2.37 | −0.12 |
| 19252571+0031444 | *CoRoT* | 19:25:25.71 | +00:31:44.4 | 12.7 | 11.9 | $-38.6 \pm 0.3$ | 4825 | 2.87 | −0.10 |
| 19252758+0153065 | *CoRoT* | 19:25:27.58 | +01:53:06.5 | 11.3 | 10.5 | $28.2 \pm 0.1$ | 4617 | 2.80 | 0.21 |
| 19252837+0027037 | *CoRoT* | 19:25:28.37 | +00:27:03.7 | 13.4 | 12.6 | $0.3 \pm 0.3$ | 4731 | 2.91 | 0.18 |
| 19253819+0031094 | *CoRoT* | 19:25:38.19 | +00:31:09.4 | 13.0 | 12.1 | $26.6 \pm 0.3$ | 4655 | 2.51 | −0.25 |
| 19261007−0010200 | *CoRoT* | 19:26:10.07 | −00:10:20.0 | 11.8 | 11.1 | $-21.6 \pm 0.2$ | 4752 | 2.84 | 0.12 |
| 19264038−0019575 | *CoRoT* | 19:26:40.38 | −00:19:57.5 | 13.0 | 12.2 | $41.8 \pm 0.3$ | 4782 | 2.91 | 0.02 |
| 19301883−0004175 | *CoRoT* | 19:30:18.83 | −00:04:17.5 | 11.6 | 10.5 | $57.3 \pm 0.1$ | 4070 | 1.63 | −0.52 |

**Table 2.** Positions, photometry, velocities and stellar parameters for all Li-rich stars in the sample. Candidates observed with UVES are at the head of the table, separated from the GIRAFFE spectra by the horizontal line.

| Element | Ion | A(X) | $\sigma$ | [X/H] | [X/Fe] |
|---|---|---|---|---|---|
| 08110403-4852137 | | | | | |
| Ti | 1 | 4.82 | ··· | −0.08 | 0.04 |
| Co | 1 | 4.82 | ··· | −0.10 | 0.02 |
| 19230935+0123293 | | | | | |
| Al | 1 | 6.48 | 0.05 | 0.11 | 0.23 |
| Si | 1 | 7.61 | 0.04 | 0.10 | 0.22 |
| Ca | 1 | 6.12 | 0.10 | −0.19 | −0.07 |
| Ti | 1 | 4.94 | ··· | 0.04 | 0.16 |
| Co | 1 | 4.77 | ··· | −0.15 | −0.03 |
| Ni | 1 | 6.19 | 0.03 | −0.04 | 0.08 |
| Ba | 2 | 1.81 | 0.25 | −0.36 | −0.24 |
| 19252571+0031444 | | | | | |
| Al | 1 | 6.29 | 0.12 | −0.08 | 0.02 |
| Si | 1 | 7.36 | 0.02 | −0.15 | −0.05 |
| Ca | 1 | 5.97 | 0.01 | −0.34 | −0.24 |
| Ti | 1 | 4.71 | ··· | −0.19 | −0.09 |
| Co | 1 | 4.75 | ··· | −0.17 | −0.07 |
| Ni | 1 | 5.82 | 0.02 | −0.41 | −0.31 |
| Ba | 2 | 2.20 | 0.08 | 0.03 | 0.13 |
| 19252758+0153065 | | | | | |
| Mg | 1 | 7.84 | 0.01 | 0.31 | 0.10 |
| Al | 1 | 6.68 | 0.03 | 0.31 | 0.10 |
| Si | 1 | 7.73 | 0.03 | 0.22 | 0.01 |
| Ti | 1 | 5.10 | ··· | 0.20 | −0.01 |
| Mn | 1 | 5.48 | 0.04 | 0.09 | −0.12 |
| Fe | 1 | 7.71 | 0.02 | 0.26 | 0.05 |
| Co | 1 | 4.92 | ··· | 0.00 | −0.21 |
| 19252837+0027037 | | | | | |
| Ti | 1 | 4.86 | ··· | −0.04 | −0.22 |
| Co | 1 | 4.93 | ··· | 0.01 | −0.17 |
| 19253819+0031094 | | | | | |
| Ti | 1 | 4.69 | ··· | −0.21 | 0.04 |
| Co | 1 | 4.52 | ··· | −0.40 | −0.15 |
| Ba | 2 | 1.84 | 0.11 | −0.33 | −0.08 |
| 19261007-0010200 | | | | | |
| Ti | 1 | 4.64 | ··· | −0.26 | −0.38 |
| Co | 1 | 4.77 | ··· | −0.15 | −0.27 |
| 19264038-0019575 | | | | | |
| Ti | 1 | 4.65 | ··· | −0.25 | −0.27 |
| Co | 1 | 4.78 | ··· | −0.14 | −0.16 |
| 19301883-0004175 | | | | | |
| Mg | 1 | 7.48 | 0.01 | −0.05 | 0.47 |
| Al | 1 | 6.23 | 0.01 | −0.14 | 0.38 |
| Si | 1 | 7.13 | 0.07 | −0.38 | 0.14 |
| Ca | 2 | 6.12 | 0.07 | −0.19 | 0.33 |
| Ti | 1 | 4.68 | 0.02 | −0.22 | 0.30 |
| Ti | 2 | 4.81 | 0.06 | −0.09 | 0.43 |
| Cr | 1 | 5.13 | 0.06 | −0.51 | 0.01 |
| Mn | 1 | 4.77 | 0.19 | −0.62 | −0.10 |
| Fe | 1 | 7.02 | 0.02 | −0.43 | 0.09 |
| Co | 1 | 4.47 | 0.02 | −0.45 | 0.07 |

**Table 3.** Chemical abundances (except Li, see Table 5) for all Li-rich stars observed with GIRAFFE. Note that seven stars observed with GIRAFFE have no detailed chemical abundances available.

| Species | | A(X) | $\sigma$ | [X/H] | [X/Fe] | A(X) | $\sigma$ | [X/H] | [X/Fe] |
|---|---|---|---|---|---|---|---|---|---|
| | | 08095783 − 4701385 | | | | 18033785 − 3009201 | | | |
| C | 1 | ... | ... | ... | ... | 8.50 | 0.18 | 0.11 | 0.04 |
| O | 1 | ... | ... | ... | ... | 8.74 | 0.12 | 0.08 | 0.01 |
| Na | 1 | 6.12 | 0.03 | −0.05 | 0.10 | 6.53 | 0.05 | 0.36 | 0.29 |
| Mg | 1 | 7.49 | 0.04 | −0.04 | 0.11 | 7.91 | 0.12 | 0.38 | 0.31 |
| Al | 1 | 6.25 | 0.01 | −0.12 | 0.03 | 6.68 | 0.07 | 0.31 | 0.24 |
| Si | 1 | 7.30 | 0.01 | −0.21 | −0.06 | 7.52 | 0.07 | 0.01 | −0.06 |
| S | 1 | ... | ... | ... | ... | 7.48 | 0.07 | 0.34 | 0.27 |
| Ca | 1 | 6.07 | 0.01 | −0.24 | −0.09 | 6.35 | 0.08 | 0.04 | −0.03 |
| Sc | 1 | ... | ... | ... | ... | 3.00 | 0.09 | −0.17 | −0.24 |
| Sc | 2 | 3.08 | 0.02 | −0.09 | 0.06 | 3.29 | 0.08 | 0.12 | 0.05 |
| Ti | 1 | 4.74 | 0.06 | −0.16 | −0.01 | 4.95 | 0.08 | 0.05 | −0.02 |
| Ti | 2 | 4.73 | 0.02 | −0.17 | −0.02 | 5.01 | 0.09 | 0.11 | 0.04 |
| V | 1 | ... | ... | ... | ... | 4.12 | 0.08 | 0.12 | 0.05 |
| Cr | 1 | 5.33 | 0.03 | −0.31 | −0.16 | 5.65 | 0.11 | 0.01 | −0.06 |
| Cr | 2 | 5.35 | 0.14 | −0.29 | −0.14 | 5.88 | 0.12 | 0.24 | 0.17 |
| Mn | 1 | ... | ... | ... | ... | 5.42 | 0.16 | 0.03 | −0.04 |
| Fe | 1 | 7.20 | 0.02 | −0.25 | −0.10 | 7.52 | 0.10 | 0.07 | 0.00 |
| Fe | 2 | 7.17 | 0.06 | −0.28 | −0.13 | 7.56 | 0.09 | 0.11 | 0.04 |
| Co | 1 | ... | ... | ... | ... | 5.04 | 0.10 | 0.12 | 0.05 |
| Ni | 1 | 5.97 | 0.02 | −0.26 | −0.11 | 6.47 | 0.11 | 0.24 | 0.17 |
| Cu | 1 | ... | ... | ... | ... | 4.15 | 0.12 | −0.06 | −0.13 |
| Zn | 1 | 4.44 | 0.12 | −0.16 | −0.01 | 4.29 | 0.13 | −0.31 | −0.38 |
| Sr | 1 | 3.27 | 0.03 | 0.35 | 0.50 | 3.08 | 0.21 | 0.16 | 0.09 |
| Y | 2 | 1.82 | 0.06 | −0.39 | −0.24 | 1.96 | 0.12 | −0.25 | −0.32 |
| Zr | 1 | 2.29 | 0.02 | −0.29 | −0.14 | 2.48 | 0.13 | −0.10 | −0.17 |
| Zr | 2 | 2.37 | 0.06 | −0.21 | −0.06 | 2.55 | 0.17 | −0.03 | −0.10 |
| Mo | 1 | ... | ... | ... | ... | 1.78 | 0.15 | −0.14 | −0.21 |
| Ba | 2 | ... | ... | ... | ... | 2.06 | 0.14 | −0.11 | −0.18 |
| La | 2 | 0.73 | 0.03 | −0.40 | −0.25 | 0.91 | 0.15 | −0.22 | −0.29 |
| Ce | 2 | 1.40 | 0.08 | −0.30 | −0.15 | 1.42 | 0.14 | −0.28 | −0.35 |
| Pr | 2 | ... | ... | ... | ... | −0.19 | 0.46 | −0.77 | −0.84 |
| Nd | 2 | ... | ... | ... | ... | 1.37 | 0.18 | −0.08 | −0.15 |
| Eu | 2 | ... | ... | ... | ... | 0.64 | 0.10 | 0.12 | 0.05 |
| | | 19242472 + 0044106 | | | | 19304281 + 2016107 | | | |
| C | 1 | 8.47 | 0.13 | 0.08 | 0.00 | 8.20 | 0.13 | −0.19 | −0.09 |
| N | (CN) | 8.26 | 0.10 | 0.48 | 0.40 | ... | ... | ... | ... |
| O | 1 | 8.94 | 0.12 | 0.28 | 0.20 | 8.76 | 0.20 | 0.10 | 0.20 |
| Na | 1 | 6.51 | 0.05 | 0.34 | 0.26 | 6.25 | 0.05 | 0.08 | 0.18 |
| Mg | 1 | 7.69 | 0.12 | 0.16 | 0.08 | 7.55 | 0.12 | 0.02 | 0.12 |
| Al | 1 | 6.63 | 0.07 | 0.26 | 0.18 | 6.42 | 0.07 | 0.05 | 0.15 |
| Si | 1 | 7.52 | 0.07 | 0.01 | −0.07 | 7.41 | 0.07 | −0.10 | 0.00 |
| S | 1 | 7.21 | 0.07 | 0.07 | −0.01 | 7.06 | 0.07 | −0.08 | 0.02 |
| Ca | 1 | 6.32 | 0.08 | 0.01 | −0.07 | 6.19 | 0.07 | −0.12 | −0.02 |
| Sc | 1 | 3.36 | 0.09 | 0.19 | 0.11 | 2.98 | 0.07 | −0.19 | −0.09 |
| Sc | 2 | 3.22 | 0.06 | 0.05 | −0.03 | 3.18 | 0.07 | 0.01 | 0.11 |
| Ti | 1 | 5.05 | 0.08 | 0.15 | 0.07 | 4.76 | 0.08 | −0.14 | −0.04 |
| Ti | 2 | 5.04 | 0.07 | 0.14 | 0.06 | 4.88 | 0.09 | −0.02 | 0.08 |
| V | 1 | 4.11 | 0.08 | 0.11 | 0.03 | 3.78 | 0.08 | −0.22 | −0.12 |
| Cr | 1 | 5.72 | 0.10 | 0.08 | 0.00 | 5.40 | 0.13 | −0.24 | −0.14 |
| Cr | 2 | 5.70 | 0.14 | 0.06 | −0.02 | 5.72 | 0.15 | 0.08 | 0.18 |
| Mn | 1 | 5.41 | 0.11 | 0.02 | −0.06 | 5.23 | 0.16 | −0.16 | −0.06 |
| Fe | 1 | 7.52 | 0.09 | 0.07 | −0.01 | 7.37 | 0.10 | −0.08 | 0.02 |
| Fe | 2 | 7.47 | 0.09 | 0.02 | −0.06 | 7.48 | 0.08 | 0.03 | 0.13 |
| Co | 1 | 5.12 | 0.10 | 0.20 | 0.12 | 4.80 | 0.10 | −0.12 | −0.02 |
| Ni | 1 | 6.36 | 0.10 | 0.13 | 0.05 | 6.17 | 0.10 | −0.06 | 0.04 |
| Cu | 1 | 4.30 | 0.14 | 0.09 | 0.01 | 4.05 | 0.14 | −0.16 | −0.06 |
| Zn | 1 | 3.95 | 0.13 | −0.65 | −0.73 | 4.78 | 0.13 | 0.18 | 0.28 |
| Sr | 1 | 3.53 | 0.20 | 0.61 | 0.53 | 3.20 | 0.21 | 0.28 | 0.38 |
| Y | 2 | 2.17 | 0.11 | −0.04 | −0.12 | 2.14 | 0.12 | −0.07 | 0.03 |
| Zr | 1 | 2.55 | 0.15 | −0.03 | −0.11 | 2.56 | 0.14 | −0.02 | 0.08 |
| Zr | 2 | 2.99 | 0.10 | 0.41 | 0.33 | 2.90 | 0.10 | 0.32 | 0.42 |
| Mo | 1 | 2.15 | 0.10 | 0.23 | 0.15 | 1.72 | 0.10 | −0.20 | −0.10 |
| Ba | 2 | 2.26 | 0.14 | 0.09 | 0.01 | 2.20 | 0.14 | 0.03 | 0.13 |
| La | 2 | 1.12 | 0.15 | −0.01 | −0.09 | 0.90 | 0.16 | −0.23 | −0.13 |
| Ce | 2 | 1.70 | 0.13 | 0.00 | −0.08 | 1.59 | 0.15 | −0.11 | −0.01 |
| Pr | 2 | ... | ... | ... | ... | 0.72 | 0.29 | 0.14 | 0.24 |
| Nd | 2 | 1.83 | 0.15 | 0.38 | 0.30 | 1.37 | 0.19 | −0.08 | 0.02 |
| Eu | 2 | 0.84 | 0.13 | 0.32 | 0.24 | 0.58 | 0.10 | 0.06 | 0.16 |

**Table 4.** Detailed chemical abundances (except Li; see Table 5) for all Li-rich stars observed with UVES.

| Star | A(Li, LTE) | A(Li, nLTE) |
|---|---|---|
| 08095783−4701385 | 3.51 | 3.21 |
| 18033785−3009201 | 3.19 | 3.11 |
| 19242472+0044106 | 2.74 | 2.72 |
| 19304281+2016107 | 2.60 | 2.60 |
| 08102116−4740125 | 3.52 | 3.33 |
| 08110403−4852137 | 3.51 | 3.25 |
| 08395152−5315159 | 2.15 | 2.28 |
| 10300194−6321203 | 2.96 | 2.88 |
| 10323205−6324012 | 3.07 | 2.98 |
| 10495719−6341212 | 3.05 | 2.94 |
| 10503631−6512237 | 2.59 | 2.61 |
| 11000515−7623259 | 2.59 | 2.64 |
| 19230935+0123293 | 2.80 | 2.75 |
| 19252571+0031444 | 2.10 | 2.22 |
| 19252758+0153065 | 2.99 | 2.92 |
| 19252837+0027037 | 2.86 | 2.82 |
| 19253819+0031094 | 2.99 | 2.85 |
| 19261007−0010200 | 2.95 | 2.88 |
| 19264038−0019575 | 3.35 | 3.13 |
| 19301883−0004175 | 2.52 | 2.43 |

**Table 5.** Non-LTE Li calculated using corrections from Lind et al. (2009a). Stars observed using UVES and GIRAFFE are separated by the horizontal line. For these calculations we adopted $\xi = 1.5$ km s$^{-1}$ for the GIRAFFE spectra as $\xi$ measurements were unavailable.

[1]Institute of Astronomy, University of Cambridge, Madingley Road, Cambridge CB3 0HA, UK
[2]Lund Observatory, Department of Astronomy and Theoretical Physics, Box 43, SE-221 00 Lund, Sweden
[3]INAF - Osservatorio Astrofisico di Arcetri, Largo E. Fermi 5, 50125, Florence, Italy
[4]Max-Planck Institut für Astronomie, Königstuhl 17, 69117 Heidelberg, Germany
[5]Department of Physics and Astronomy, Uppsala University, Box 516, SE-751 20 Uppsala, Sweden
[6]Astrophysics Group, Keele University, Keele, Staffordshire ST5 5BG, United Kingdom
[7]INAF - Padova Observatory, Vicolo dell'Osservatorio 5, 35122 Padova, Italy
[8]INAF - Osservatorio Astronomico di Bologna, via Ranzani 1, 40127, Bologna, Italy
[9]INAF - Osservatorio Astronomico di Palermo, Piazza del Parlamento 1, 90134, Palermo, Italy
[10]GEPI, Observatoire de Paris, CNRS, Université Paris Diderot, 5 Place Jules Janssen, 92190 Meudon, France
[11]Dipartimento di Fisica e Astronomia, Sezione Astrofisica, Universitá di Catania, via S. Sofia 78, 95123, Catania, Italy
[12]ASI Science Data Center, Via del Politecnico SNC, 00133 Roma, Italy
[13]Laboratoire Lagrange (UMR7293), Université de Nice Sophia Antipolis, CNRS,Observatoire de la Côte d'Azur, CS 34229,F-06304
Nice cedex 4, France
[14]Department for Astrophysics, Nicolaus Copernicus Astronomical Center, ul. Rabiańska 8, 87-100 Toruń, Poland
[15]European Southern Observatory, Alonso de Cordova 3107 Vitacura, Santiago de Chile, Chile
[16]Instituto de Astrofísica de Andalucía-CSIC, Apdo. 3004, 18080 Granada, Spain
[17]Università di Bologna, Dipartimento di Fisica e Astronomia, viale Berti Pichat 6/2, 40127 Bologna, Italy
[18]INAF - Osservatorio Astrofisico di Catania, via S. Sofia 78, 95123, Catania, Italy
[19]Astrophysics Research Institute, Liverpool John Moores University, 146 Brownlow Hill, Liverpool L3 5RF, United Kingdom
[20]Departamento de Ciencias Fisicas, Universidad Andres Bello, Republica 220, Santiago, Chile
[21]Millennium Institute of Astrophysics, Chile
[22]Pontificia Universidad Católica de Chile, Av. Vicuña Mackenna 4860, 782-0436 Macul, Santiago, Chile
[23]Instituto de Astrofísica e Ciências do Espaço, Universidade do Porto, CAUP, Rua das Estrelas, 4150-762 Porto, Portugal
[24]Institute of Theoretical Physics and Astronomy, Vilnius University, A. Gostauto 12, LT-01108 Vilnius
[25]Faculty of Mathematics and Physics, University of Ljubljana, Jadranska 19, 1000, Ljubljana, Slovenia
[26]School of Physics, University of New South Wales, Sydney NSW 2052, Australia
[27]Stellar Astrophysics Centre, Department of Physics and Astronomy, Aarhus University, Ny Munkegade 120, DK-8000 Aarhus C, Denmark
[28]School of Physics and Astronomy, University of Birmingham, Edgbaston, Birmingham B15 2TT, United Kingdom
[29]Leibniz-Institut für Astrophysik Potsdam (AIP), An der Sternwarte 16, 14482 Potsdam, Germany
[30]Department of Physics and Astronomy G. Galilei, University of Padova, Vicolo dell'Osservatorio 3, I-35122 Padova, Italy
[31]Institut d'Astrophysique et de Géophysique, Université de Liège, Quartier Agora, Bât. B5c, Allée du 6 Août, 19c 4000 Liège, Belgium